SIGNAL RECONSTRUCTION FROM NONUNIFORM SAMPLES

A THESIS SUBMITTED TO
THE GRADUATE SCHOOL OF NATURAL AND APPLIED SCIENCES
OF
MIDDLE EAST TECHNICAL UNIVERSITY

BY

BÜLENT SERDAROĞLU

IN PARTIAL FULFILLMENT OF THE REQUIREMENTS
FOR
THE DEGREE OF MASTER OF SCIENCE

IN

ELECTRICAL AND ELECTRONICS ENGINEERING

JANUARY 2005

Approval of the Graduate School of Natural and Applied Sciences

Prof. Dr. Canan Özgen

Director

I certify that this thesis satisfies all the requirements as a thesis for the degree of Master of Science

Prof. Dr. İsmet Erkmen

Head of Department

This is to certify that we have read this thesis and that in our opinion it is fully adequate, in scope and quality, as a thesis for the degree of Master of Science

Assoc. Prof. Dr. Temel Engin Tuncer

Supervisor

Examining Committee Members

Prof. Dr. Nevzat Gencer (METU/EEE) _____

Assoc. Prof. Dr. Temel Engin Tuncer (METU/EEE) _____

Assoc. Prof. Dr. Tolga Çiloğlu (METU/EEE) _____

Assoc. Prof. Dr. Aydın Alatan (METU/EEE) _____

Assist. Prof. Dr. Yakup Özkazanç (Hacettepe Unv/EEE) _____

I hereby declare that all information in this document has been obtained and presented in accordance with academic rules and ethical conduct. I also declare that, as required by these rules and conduct, I have fully cited and referenced all material and results that are not original to this work.

Bülent Serdaroğlu :

Sign :

ABSTRACT

SIGNAL RECONSTRUCTION FROM NONUNIFORM SAMPLES

Serdaroğlu, Bülent
M.S., Electrical and Electronics Engineering Department
Supervisor : Assoc. Dr. Temel Engin Tuncer

January 2005, 91 pages

Sampling and reconstruction is used as a fundamental signal processing operation since the history of signal theory. Classically uniform sampling is treated so that the resulting mathematics is simple. However there are various instances that nonuniform sampling and reconstruction of signals from their nonuniform samples are required. There exist two broad classes of reconstruction methods. They are the reconstruction according to a deterministic, and according to a stochastic model. In this thesis, the most fundamental aspects of nonuniform sampling and reconstruction, according to a deterministic model, is analyzed, implemented and tested by considering specific nonuniform reconstruction algorithms. Accuracy of reconstruction, computational efficiency and noise stability are the three criteria that nonuniform reconstruction algorithms are tested for. Specifically, four classical closed form interpolation algorithms proposed by Yen are discussed and implemented. These algorithms are tested, according to the proposed criteria, in a variety of conditions in order to identify their performances for reconstruction quality and robustness to noise and signal conditions. Furthermore, a filter bank approach is discussed for the interpolation from nonuniform samples in a computationally efficient manner. This approach is

implemented and the efficiency as well as resulting filter characteristics is observed. In addition to Yen's classical algorithms, a trade off algorithm, which claims to find an optimal balance between reconstruction accuracy and noise stability is analyzed and simulated for comparison between all discussed interpolators. At the end of the stability tests, Yen's third algorithm, known as the classical recurrent nonuniform sampling, is found to be superior over the remaining interpolators, from both an accuracy and stability point of view.

Keywords: nonuniform, sampling, reconstruction

ÖZ

DÜZGÜN OLMAYAN ÖRNEKLERİNDEN SİNYAL YAPILANDIRMASI

Serdaroğlu, Bülent
Master, Elektrik ve Elektronik Mühendisliği Bölümü
Tez Yöneticisi : Doç. Dr. Temel Engin Tuncer

Ocak 2005, 91 sayfa

Örnekleme ve yeniden yapılandırma, sinyal teorisi tarihinin başından bu yana uygulanan en temel sinyal işleme operasyonlarındandır. Düzgün örnekleme sonuçta ulaşılan matematik basit olduğu için klasik olarak incelenmiştir. Ancak öyle durumlar mevcuttur ki sinyallerin düzgün olmayan örneklenmesi ve bu örneklerden yeniden üretilmesi gerekebilmektedir. Temelde iki çeşit interpolasyon metodu mevcuttur, bunlardan ilki deterministik bir modele göre interplolasyon yaparken ikincisi ise stokastik bir modele göre interpolasyon yapmaktadır. Bu tezde ,deterministik bir modele göre işleyen, düzgün olmayan örneklemenin ve interpolasyonun en temel yönleri, spesifik düzgün olmayan örnekleme algoritmaları kullanılarak, muhtemel birçok açıdan analiz ve test edildi. Interpolasyon doğruluğu, işlemsel verimlilik ve gürültüye karşı dayanıklılık düzgün olmayan örnekleme algoritmalarının test edilmesi için kullanılan üç temel kriterdir. Bu tezde Yen tarafından önerilen, dört klasik kapalı hal interpolasyon algoritması tartışılıp uygulandı. Bu algoirtmalar, sözü edilen kriterler ışığında, birçok şart altında, interpolasyon kalitelerini ve gürültü ve sinyal tipine karşı dayanıklılıklarını tanımlamak için tartışılıp test edildi. Ayrıca düzgün olmayan

örneklerden verimli bir şekilde interpolasyon yapabilmeyi sağlayan filtre bankası yöntemi tanıtılıp tartışıldı. Bu yöntem uygulanıp, verimlilik ve ortaya çıkan filtre karakteristikleri gözlemlendi. Yen'in algoritmalarına ek olarak, gürültü dayanıklılığı ve interpolasyon doğruluğu arasında optimal bir seçim yaptığını öne süren bir arayol algoritması , daha once tanıtılan interpolatörler ile kıyaslamak için tanımlanıp simüle edildi. Gürültü dayanıklılığı testlerinin sonucunda, Yen'in periyodik düzgün olmayan örnekleme olarak bilinen, üç numaralı algoritması, hem doğruluk hem de dayanıklılık açısından diğer interpolatörlere kıyasla mükemmel olarak bulunmuştur.

Anahtar Kelimeler: Düzgün olmayan, örnekleme, yeniden yapılandırma

To my family,

My mother Bahriye, deceased father Halim, and sisters Nuray and Eray

ACKNOWLEDGMENTS

I would like to express my gratitude to Assoc. Prof. Temel Engin Tuncer of electrical and electronics engineering department, for his support of the work, even under situations difficult to do so. His support was an invaluable experience, which I have gained throughout the completion of the work.

I would also like to thank to the academic staff of METU for they have let me pave my way through my engineering education.

TABLE OF CONTENTS

CHAPTER 1

INTRODUCTION

In the study of sampling and reconstruction, there exist three main criteria to judge a given strategy and its corresponding reconstruction algorithm. They are the reconstruction accuracy, computational efficiency and noise stability. The criterions will be treated in their corresponding chapters. In this introduction, a solid background of interpolation theory and its application into nonuniform sampling will be given so that some necessary mathematical details are presented.

1.1 Analysis of interpolation theory

1.1.1 Lagrangian interpolation

According to the references [1] and [2], interpolation theory can be traced back into the works of Lagrange. Lagrangian interpolation is the first systematic approach to define interpolation as a mathematical tool. It can be seen from the reference [2] that, the form of interpolating polynomial summation can evolve into the more familiar interpolation series, upon which sampling and reconstruction can be raised. A Lagrangian polynomial is the following function

$$P_n(t) = f_0 L_0^n(t) + f_1 L_1^n(t) + ... + f_n L_n^n(t) \qquad (1.1a)$$

Where $f_n = f(t_n)$ are the sample values of the function $f(t)$ and the so

called Lagrangian coefficients, denoted by $L_i^n(t)$, are given as

$$L_i^n(t) = \frac{(t-t_0)(t-t_1)...(t-t_{i-1})(t-t_{i+1})...(t-t_n)}{(t_i-t_0)(t_i-t_1)...(t_i-t_{i-1})(t_i-t_{i+1})...(t_i-t_n)} \tag{1.1b}$$

Henceforth the equation (1.1a) interpolates the values of function $f(t)$ according to its samples $f_n = f(t_n)$ with the help of the composing functions, denoted as $L_i^n(t)$. (Though they are called as the interpolation coefficients, actually they are the interpolation basis functions and the sample values of the functions are the weighting coefficients.)

In order to further manipulate the Lagrangian interpolation, the Lagrangian coefficient can be written as follows. Let $g_n(t)$ be defined as

$$g_n(t) = (t-t_0)(t-t_1)...(t-t_n) \tag{1.2}$$

Then the Lagrangian coefficients can be written in the form of

$$L_i^n(t) = \frac{g_n(t)}{(t-t_i)g_n'(t_i)} \tag{1.3}$$

and the Lagrangian interpolation polynomial becomes

$$P_n(t) = g_n(t)\sum_{i=0}^{n}\frac{f_i}{(t-t_i)g_n'(t_i)} \tag{1.4}$$

When n goes to infinity, this will become as the infinite length interpolator that forms the link between bandlimited and polynomial interpolation.

1.1.2. Whittaker series interpolation

E.T. Whittaker in [5] and J.M. Whittaker in [6] set out to find an analytic expression for a function when the values of the function are known for equidistant values of its argument. Stating that this expression is free of periodic components with a period less than $2w$, the resulting function was called as the *Cardinal Function.*

E.T. Whittaker showed that this analytic expression is both an interpolatory and a representative one. The representative indication was a point that later Shannon used in his theorem as a starting point. More specifically what Whittaker considered could be stated as below.

Theorem 1.1:

" Consider a function, which is assumed to have no periodic components with period less than 2w. This function can be represented by its samples taken at the values of its argument spaced uniformly. Considering the sample values of the function $f(t)$, as $f(a), f(a+w), f(a+2w),...., f(a+nw),....$then the cardinal function can be expressed in terms of its samples as follows."

$$f(t) = \sum_{n=-\infty}^{\infty} f(a+nw) \frac{\sin(\frac{\pi}{w}(t-a-nw))}{\frac{\pi}{w}(t-a-nw)} \qquad (1.5)$$

The above representation of the cardinal function, $f(t)$, was in terms of an infinite sum and mathematically it was called as the *cardinal series*. Looking at the series carefully it is apparent that this form was the one that Shannon and Nyquist used in their theories, where the term cardinal series became as interpolation summation. The above cardinal series is what is sometimes called as the Whittaker's sampling theorem.

At this point, it is worth noting that both Lagrangian interpolation and Whittaker series were used in the field of mathematics for interpolation of functions from their values. There was no indication of an engineering interest in the sampling theorem for the purpose of using it as a tool for communication or signal processing theory. The first remarkable reference to interpolation theory as a signal sampling theorem was set by Nyquist [4].

1.1.3 Nyquist sampling theorem

Nyquist, in his paper [4] made a remarkable addition to the communication literature. Well known with his contributions to the telegraph transmission theory, Nyquist eventually discovered sampling as a necessity for digital signal communication, (known as telegraph pulse modulation and transmission in his time). Nyquist, using a modified form of Whittaker series, set out two important remarks on sampling theorem.

The first is the fact that a signal bandlimited to W hz should be sampled at a rate larger than $2W$, in order to be transmitted correctly and uniquely over communication lines. Where the $2W$ frequency of sampling is inserted into the literature as the Nyquist rate and the W frequency as the Nyquist frequency. And secondly he gave a proof of the sampling theorem, by using the Fourier series expansions of the signals considered. This fact, the use of Fourier series of the signal to prove the sampling theorem of bandlimited signals was first attributed to Nyquist in history and therefore the theorem of sampling is initially named as the Nyquist sampling theorem. Although the mechanics of sampling and reconstruction that Nyquist used, were a replica of what Whittaker series was. More on the history of sampling theorem can be found in the references [26] , [27] as historical treatment.

1.1.4 Shannon sampling theorem

One of the most reputable papers on sampling theory belongs to C.E. Shannon [3]. Shannon was the first to conceptually prove the sampling theorem in a neat way by introducing the Fourier domain of the signal into the case. Shannon also considered the integral transform visualization of sampling and used the Fourier transform as a special case. This is the reason why the classical sampling theorem is called as the "Shannon sampling theorem". Shannon's original statement of the sampling theorem is the following:

Theorem 1.2:

" If a function $f(t)$ contains no frequencies higher than W cps, it is completely determined by giving its ordinates at a series of points spaced 1/2W s apart. "

The reconstruction of the function $f(t)$, as a sampling series, is given by Shannon according to the following summation.

$$f(t) = \sum_{n=-\infty}^{\infty} f(\frac{n}{2W}) \frac{\sin(\pi(2Wt-n))}{\pi(2Wt-n)} \tag{1.6}$$

The reconstruction formula is the same with the Whittaker series and the Nyquist interpolation. A proof of this theorem is given in [3]. It is based on the Fourier transform of the signal and its Fourier series expansion. Shannon also made an important remark on the type of sampling. According to [3], the signal can be reconstructed even if the samples are taken at nonuniform instants. The exact distribution of those nonuniform instants is arbitrary. They should however satisfy the condition that the average sampling rate is still at least the Nyquist rate. Where the average sampling rate is defined as the temporary mean of the instantaneous sampling rate function, evaluated throughout the sampling process.

1.1.5 Definition of nonuniform sampling

In the previous sections, sampling theorem has been investigated in its chronological development. Most of the literature about sampling deals with a uniform grid. However it is also possible to use nonuniform grids. When nonuniform sampling strategies are employed, both processes of sampling and reconstruction become more complicated and involved. In addition, it should be noted that unlike the simple uniform sampling case, there is no unique theory that explicitly expresses the interpolation equation for any given nonuniform sampling grid. Nevertheless, there exists a generalized sampling theorem that expresses the general outlines of reconstruction procedure for any given sampling strategy. And also the Lagrangian interpolation remains valid under nonuniform sample point distributions as well as the uniform case.

Throughout this thesis, different kinds of nonuniform sampling grids are used. Strictly speaking there are infinitely many different nonuniform sampling grids, each having their own type of reconstruction formulas. The variety of reconstruction formulas directly stems from the variety of sampling grids. However, still three broad classes of nonuniform sampling grids can be defined.

1-Analytically definable sampling grid
2-Completely random sampling grid
3-A mix of 1 and 2 in a forced (probably periodic) structure.

The first class of grids has the property that every sampling instant can be defined explicitly with its given sampling index. (i.e. given the sequence of samples and an arbitrary initial instant value, the rest of sampling instants can be derived just from the sequence index) A Bessel function can be a good example of such a nonuniform analytic grid. The zero crossings of the Bessel function, which are nonuniformly occurring in the argument of the function, define the sampling instants.

The second class of the grids has the obvious property that they have no closed form analytic structure. The sampling instants are distributed with a given probabilistic model. The simplest of such a distribution can be a Gaussian, a uniform or an arbitrary white distribution model. It is interesting to note that if we can sample not only the signal but also the argument of the signal (time or space) then the reconstruction procedure has almost the same complexity compared to the analytic case.

In many applications the second class grids will find more value. Because, the natural cause of nonuniformities will come from the randomness of nature itself, which will directly impose the randomness of the sampling instant distributions. At this point two different approaches to the second class nonuniform sampling grids should be mentioned.

A) Random sampling with known sampling instants.
B) Random sampling with unknown sampling instants.

The first case sampling strategy has the property that in reconstruction, we can use the information of sampling instants. This is indeed the most vital requirement of all deterministic sampling strategies. This can be seen from the following fact. The Lagrangian interpolation uses the most basic idea of curve fitting for a given set of points. This method can only work if the both coordinates of the points are exactly known. Any error in those coordinates will result in an error in the interpolation and a complete loss of ordinate information will result in a fatal error of interpolation. In fact, interpolation will not be possible at all. Therefore, it can be stated without proof that all sampling strategies, which have an inheritance from the Lagrangian interpolation, assume that both the sample values and the sampling instants are known for the interpolation to work. No interpolation is possible, otherwise, without any extra information.

What can be done for the case where the sampling instants are not known? It is apparent that exact interpolations based on the deterministic models will not work. Only an approximate solution can be expected from a Lagrangian interpolator under such a circumstance. And even the whole process is suspicious, since infinitely many different signaling conditions can produce the same set of samples, if the sampling instants are not strictly defined. The only improvement on the interpolation may come from a probabilistic model assumption of the sampling process. There exist known results for such a distribution of samples. More details can be found in [9], [10] and [11] for a complete treatment of interpolation from random samples without the sampling instants. The key property of the reconstruction procedure is the fact that the sampling instants are assumed to obey a given pdf. This fact improves the reconstruction process from a completely unknown sampling instant set.

Of course, it is obvious that a probabilistic model for reconstruction of a signal from its completely random samples will bring an unavoidable error to the interpolation. The magnitude of this error depends on the ability to predict the sampling instants, (or the sample values), for a given pdf. The better the prediction the better is the interpolation.

The last class of sampling grids is a mixture of class one and two. The mix has the property that it is in general an artificial sampling grid. The reconstruction procedure, for such an artificially generated sampling instant distribution, can be derived from that of the completely random distribution case. However the structure of the grid will evidently result in a more compact reconstruction formula than the completely arbitrary case. For more details on general nonuniform sampling expansions [29] and [30] can be searched. Also [31] concentrates on iterative nonuniform reconstruction methods, which are not treated in this thesis. [32] can also be suggested for a brief example on nonuniform reconstruction. Interpolation from frequency domain concepts instead of time domain can be exemplified by [33] and [34].

1.1.6 Explicit reconstructors from nonuniform samples

The exact expressions of the closed form interpolation formulas from nonuniform samples depend on the type of sampling grid being considered. If a nonuniform sampling grid falls in class 1, then the theoretic closed form expression of interpolation can be found by a powerful theorem called as the generalized sampling theorem, (GST), which is explained in the next section. However when a sampling grid falls in class 2 or 3, the GST will not in general provide a useful solution. Under such circumstances, which are indeed occurring more than the class 1 case, special forms of Lagrangian interpolation can be used both as a numerical tool and, if possible, as a tool that lets the conversion into a closed form expression. The details of such an operation is provided in appendices A and B

1.2 Generalized sampling theorem (GST)

This section develops the required mathematical details of sampling theory. Parts of this section are summarized from reference [1], and unless otherwise stated can be reached from the corresponding papers.

The sampling theorem that is referred to Whittaker, Kotelnikov and Shannon is called as the WKS sampling theorem, which specifically deals with integral transforms that are truncated inverse Fourier integrals. Although Whittaker suggested integrals besides the Fourier, the formal details have been stated in the papers of Weiss [12] first. Then comes the work of Kramer [13] who analyzed the general integral transforms and established the generalized sampling theorem. In the literature, the generalized sampling theorem that deals with most general integral transforms is referred to as WKSK sampling theorem, where K stands for the Kramer as the last letter.

1.2.1 The generalized sampling theorem (GST)

Theorem 1.3:

"Let I be an interval and $L_2(I)$ be the class of functions $\phi(x)$ for which $\int_I |\phi(x)|^2 dx < \infty$ Suppose that for each real t

$$f(t) = \int_I K(x,t)g(x)dx \tag{1.7}$$

where $g(x) \in L_2(I)$. Suppose that for each real $t, K(x,t) \in L_2(I)$ and there exist a countable set $E = \{t_n\}$ such that $\{K(x,t_n)\}$ is a complete orthogonal set on I. Then

$$f(t) = \lim_{N\to\infty} \sum_{|n|\le\infty} f(t_n)S_n(t) \tag{1.8}$$

where

$$S_n(t) = S(t,t_n) = \frac{\int_I K(x,t)\overline{K(x,t_n)}dx}{\int_I |K(x,t_n)|^2 dx} \tag{1.9}$$

In these expressions the terms are defined as follows:

$f(t)$	: The signal that is sampled.
$K(x,t)$	: The kernel of the Integral Transform.
$g(x)$	: Transform domain representation of $f(t)$
$K(x,t_n)$	: The Kernel, evaluated at Sampling instant t_n
$S(t,t_n)$	: Interpolating function as a function of n, sample index.
t_n	: Sampling Instants

Not every integral transform is acceptable for a sampling kernel. Kramer [13] shows that the conditions on the integral transform kernel $K(x,t)$ in equation (1.7) are exhibited by the solutions of the nth order self-adjoint differential equations. Other works on the conditions of the kernel and different integral transform solutions can be found in [14], [15], [16]. For example [15] analyses the prolate spheroidal wave functions as integral transform kernels.

1.2.2 The use of GST

The WKSK describes the necessary mechanics that is required for a general integral transform based sampling system. This part will demonstrate in a step by step manner the application guideline of the theorem.

1- Define an integral transform, $K(x,t)$, that satisfies the requirements of WKSK. The integral kernels that are allowed to be used in the GST construction should posses certain properties, because they will directly affect the behavior of the interpolation kernel $S(t,t_n)$. Not every integral transform can be used, the most general study of the conditions on the integral transform, $K(x,t)$, is studied in Kramer's work [9]. One set of an example is that the kernels that satisfy the Strum-Liouville differential equations.

2- Find the interpolation function, $S(t,t_n)$. Using equation (1.9), evaluate the integrals and find a closed form explicit equation for the interpolation function $S(t,t_n)$ (also called as the composing function). At this point, theoretically, the interpolation kernel is obtained, however the integrals in (1.9) might not always be explicitly evaluated. Apart from the techniques of finding solutions to (1.9) for all possible inputs, we may use the most fundamental interpolation theorem, the Lagrangian interpolation, where (1.9) is too complex to evaluate or the corresponding $K(x,t)$ could not be found for a given nonuniform sampling distribution.

3- Define the sampling instants, hence the sampling strategy of interpolation. When an explicit formula of $S(t,n)$ is available, the sampling instants t_n are defined as the zero crossings of $S(t,n)$. That is to say $S(t_n,n)=0$ for all t_n.

The remaining step is that signal should be sampled according to the sampling instants t_n. The interpolation equation is given in (1.8). Using (1.8.) the continuous signal can be reconstructed from its samples.

1.2.3 Uniform sampling derived from WKSK

One application of the WKSK is the well known uniform sampling and the associated reconstruction formula. This example shows how to apply WKSK with an analytic transform kernel, and it will also show that uniform sampling can be derived from WKSK.

Step 1:

The integral transform that is used is the Fourier Transform; in fact, the inverse Fourier transform will be used as the integral transform. The transform pair is the following:

$$X(w)=\int_{-\infty}^{\infty}x(t)e^{-jwt}dt \qquad \text{Fourier Transform}$$

$$x(t)=\frac{1}{2\pi}\int_{-\infty}^{\infty}X(w)e^{jwt}dw \qquad \text{Inverse Fourier Transform}$$

Step 2:

From the inverse Fourier transform, the kernel of the integral transform is e^{jwt}. Note that the constant scaling factor $1/2\pi$ will be omitted since in the theory it can be integrated into the function $X(w)$.

Hence:

$$K(x,t) = K(w,t) = e^{jwt}$$

Note that x and w are replaced.

Step 3:

The kernel function e^{jwt} evaluated at the uniform sampling instant $t_n = nT$, as e^{jwnT} form a complete orthogonal set defined on $I = (-\pi/T, \pi/T)$. Therefore it meets the criterion for being a valid candidate of the kernel of integral transform that is to be used in generalized sampling theorem. The other requirements that the uniform transform kernel meets can be found from Kramer [13].

Step 4:

The remaining step is the evaluation of equation (1.9), hence the composing function $S(t,t_n)$ is

$$S(t,t_n) = \frac{\int_I e^{jwt} e^{-jwnT}\, dw}{\int_I \left| e^{jwnT} \right|^2 dw} = \frac{\int_{-\pi/T}^{\pi/T} e^{jw(t-nT)} dw}{\int_{-\pi/T}^{\pi/T} 1\, dw} \qquad (1.10)$$

The interval of transform integration is set to be $I = [-\pi/T, \pi/T]$. Because the signals that are going to be sampled and reconstructed by this interpolator assumes a bandwidth of $1/2T$ and hence the inverse Fourier transform is truncated to that band. Evaluating the integrals yields the following uniform sampling interpolator.

$$S(t,t_n) = \frac{\sin(\pi \frac{(t-nT)}{T})}{\pi \frac{(t-nT)}{T}} = \sin c(\frac{t-nT}{T}) \qquad (1.11)$$

The form of the interpolating function is the well known sinc function. When a bandlimited signal x (t) is sampled by a uniform sampling grid, with the sampling times denoted as $t_n = t = nT$, we can reconstruct the original signal from its samples $x(nT) = x[n]$, by using the formula shown below:

$$x(t) = \sum_{n=-\infty}^{\infty} x(t_n) S(t, t_n) = \sum_{n=-\infty}^{\infty} x(nT) \sin c(\frac{t - nT}{T}) \qquad (1.12)$$

using the sampled function sequence x[n] instead of x(nT) the final form is obtained for uniform sampling interpolation

$$x(t) = \sum_{n=-\infty}^{\infty} x[n] \frac{\sin(\pi \frac{(t - nT)}{T})}{\pi \frac{(t - nT)}{T}} = \sum_{n=-\infty}^{\infty} x[n] \sin c(\frac{t - nT}{T}) \qquad (1.13)$$

1.2.4 Nonuniform sampling derived from WKSK

To show that WKSK indeed solves any proper sampling kernel, a nonuniform example is treated as a special case. The result is summarized from [1]. Let $K(w,t) = J_m(wt)$ where $J_m(wt)$ is the Bessel function of the first kind of order m. For the illustration let us use a finite limit (truncated) Bessel transform.

$$x(t) = \int_0^1 w J_m(wt) X(w) dw \qquad (1.14)$$

Where $X(w)$ represents the Transform domain pair of $x(t)$. Then the interpolation function $S(t, t_n)$ is derived from the integral in (1.9) as

$$S_n(t) = S(t, t_{m,n}) = \frac{\int_0^1 wJ_m(wt)J_m(wt_{m,n})dw}{\int_0^1 w[J_m(wt)]^2 dw} = \frac{2t_{m,n}J_m(t)}{(t_{m,n}^2 - t^2)J_{m+1}(t_{m,n})} \quad (1.15)$$

where $\{t_{m,n}\}$ are the zeros of the Bessel function J_m, i.e. $J_m(t_{m,n}) = 0, n = 1,2,...$ In other words $t_{m,n}$ are the zeros of the interpolating function and they are also the sampling instants. As it is known Bessel function zeros are nonuniformly spread over its argument. Note that the linear weighting function w, is introduced explicitly in the integrals, instead of having it implicit as in the uniform sampling case.

The resulting reconstruction is as follows:

$$x(t) = \sum_{n=1}^{\infty} x(t_{m,n}) \frac{2t_{m,n}J_m(t)}{(t_{m,n}^2 - t^2)J_{m+1}(t_{m,n})} \quad (1.16)$$

Bessel function sampling is useful in many contexts, finding applications in the areas of optics, circular symmetric sampling grids, biomedical imaging and in general for the conversion of a corresponding nth order Fourier transform into a single order Bessel transform with appropriate order and kind, where the transforms are defined for the sampling strategies under concern.

CHAPTER 2

NONUNIFORM SAMPLING

In this chapter, Yen's four classical nonuniform sampling and reconstruction algorithms are introduced. The focus will be on the reconstruction quality of those classical algorithms. Different signal types and different sampling strategies will be imposed on the interpolators so that their reconstruction performances can be observed and compared to each other. The signal types that will be inputted include a practically time and bandwidth limited signal, a chirp and a truncated cosine signal. The effects of the specific nonuniform sampling grid on the accuracy of interpolation will also be tested. An extension to sample point distribution, specifically, missing sample case will also be demonstrated.

2.1 Closed form algorithms for nonuniform reconstruction

Nonuniform sampling and interpolation was known as far as uniform sampling, however the first remarkable closed form nonuniform interpolators were suggested by the classical work of Yen [17]. Since then researchers have given their attention to the subject of nonuniform sampling and interpolation. Yen analyses four different types of nonuniform sample distributions and outlines their corresponding explicit reconstruction formulas. His work is based on 2^{nd} and 3^{rd} classes of the sampling grids (see sec.1.1.4). Henceforth the explicit reconstruction formulas that are represented in [17] cannot be derived from the generalized sampling theorem.

Although Yen did not present an explicit derivation of the respective reconstruction formulas that he proposed to be correct. They can be derived in a number of contexts, however only the derivation of the 3rd algorithm will be given, to represent an example, from another reference [18] in the appendix B.

The algorithms that are analyzed in Yen's paper are shortly named as:
YEN 1: Finite number of nonuniform samples, (FNS)
YEN 2: Semi infinite nonuniform samples, (SINS)
YEN 3: Recurrent nonuniform samples, (RNS)
YEN 4: Arbitrary nonuniform samples, (ANS)

Each nonuniform reconstruction algorithm is differentiated from the others by means of its corresponding nonuniform sampling instant distribution. The easiest way of describing a sample point (instant) distribution is made by a map called the "grid map". The grid map can be described as follows:

The grid map consists of two lines; the upper line represents the uniform sampling instants at the Nyquist rate. The lower line represents the nonuniform sampling instants at the average Nyquist rate. The lines connecting the points between the upper and lower lines are there to show the migration of uniform sampling instants into their new nonuniform locations. The sampling time indicator for the upper line is the same as with the uniform sampling timings. The sampling time indicators for the lower line are generated for the nonuniform case and it can take different forms depending on the specific application.

2.1.1 Finite number of nonuniform samples, FNS, (Yen 1)

Definition of sampling strategy:

From a uniform sample point distribution a finite number of N points are migrated to new nonuniform sampling locations. The resulting grid map consists of a finite number of nonuniform points embedded in an infinite number of uniform samples.

Grid Map:

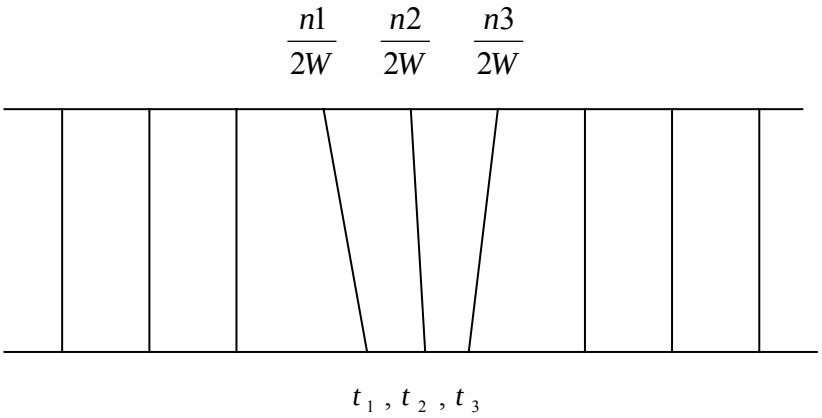

Conditions on distribution:

The number of immigrant points should stay finite. Distributions are completely random.

Expression of the distribution:

The new nonuniform sampling instants are labeled as $t_p, p = 1,2,...,N$. The corresponding uniform sampling point indexes are labeled as $n_p, p = 1,2,...,N$. Where each element of n_p is the corresponding uniform sample index for the p^{th} nonuniform point.

Theorem 2.1 [Yen 1]:

If a finite number of uniform sample points in a uniform distribution are migrated to new distinct positions $t = t_p$, thus forming a new distribution denoted by $t = \tau_m$, the bandwidth limited signal remains uniquely defined. The reconstruction of the signal is

$$f(t) = \sum_{m=-\infty}^{\infty} f(\tau_m)\Psi_m(t) \tag{2.1}$$

Where the composing function is conditionally defined as

$$\Psi_m(t) = \frac{\prod_{q=1}^{N}(t - t_q)}{\prod_{q=1}^{N}(t - \frac{nq}{2W})} \frac{\prod_{q=1}^{N}(\frac{n}{2W} - \frac{n_q}{2W})}{\prod_{q=1}^{N}(\frac{n}{2W} - t_q)} \frac{(-1)^n \sin(2\pi Wt)}{\pi(2Wt - n)}, \qquad \tau_m = \frac{n}{2W} \neq \frac{n_q}{2W}$$

for a sampling point that belongs to a uniform instant, and

$$\Psi_m(t) = \frac{\prod_{\substack{q=1 \\ q\neq p}}^{N}(t - t_q)}{\prod_{q=1}^{N}(t - \frac{n_q}{2W})} \frac{\prod_{q=1}^{N}(t_p - \frac{n_q}{2W})}{\prod_{\substack{q=1 \\ q\neq p}}^{N}(t_p - t_q)} \frac{\sin(2\pi Wt)}{\sin(2\pi Wt_p)}, \qquad \tau_m = t_p \tag{2.2}$$

for a sampling point that belongs to a nonuniform sampling instant.

2.1.2 Semi infinite nonuniform samples, SINS (Yen 2)

Definition of sampling strategy:

This algorithm defines the nonuniformity as follows; split the infinite time axis into two semi infinite lines from the time $t = 0$ location, keep the leftmost points (the negatives) in their uniform positions and shift the whole rightmost points equally an arbitrary amount to the right or left. The resulting final grid is composed of two semi-infinitely long right and left lines with a break point at $t = 0$ location.

Grid Map:

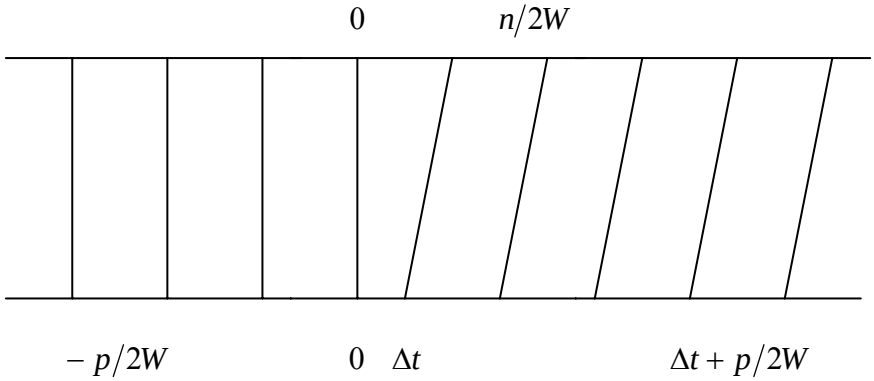

Conditions on distribution:

The parameter Δt defines the criterion on the validity of the theorem.

Case 1: $0 < \Delta t < 1/2W$

Signal is uniquely defined.

Case 2: $(M-1)/2W < -\Delta t < M/2W$ with M positive integer

Signal sample values $f(\tau_m)$ cannot be arbitrarily specified. They should satisfy M consistency conditions. Note that Δt is negative.

Case 3: $M/2W < \Delta t < (M+1)/2W$ with M positive integer

Signal is determined except for M arbitrary constants.

The last two cases are also called as *overspecifications* and *underspecifications* respectively.

Expression of the Distribution:

With the uniqueness conditions met, the sample points are denoted by τ_m with $\tau_m = -p/2W$ or $\tau_m = \Delta t + p/2W$ where $p = 0,1,2....$ as shown on the grid. For such a distribution the following theorem holds.

Theorem 2.2: [Yen 2]

If the gap Δt is positive and less than $1/2W$, the signal is uniquely specified.

The reconstruction is:

$$f(t) = \sum_{m=-\infty}^{\infty} f(\tau_m)\Psi_m(t) \tag{2.3}$$

Where the interpolation function is defined as:

$$\Psi_m(t) = \frac{(-1)^p \Gamma(2W\Delta t + p)}{\Gamma(2Wt)\Gamma[2W(\Delta t - t)]p!} \left\{ \begin{array}{l} \dfrac{1}{p+2W2}, \tau_m = -\dfrac{p}{2W} \\ \dfrac{1}{p+2W(\Delta t - t)}, \tau_m = \Delta t + \dfrac{p}{2W} \end{array} \right\} \tag{2.4}$$

2.1.3 Recurrent nonuniform samples, RNS, (YEN 3)

Definition of sampling strategy:

In this algorithm, first a group of N uniform sample points are migrated into their new locations, which are not related to each other with any analytic form. The resulting arbitrary group is then repeated infinitely in both directions of time. Hence what we obtain is a periodic, recursive structure of all nonuniform sampling instants. This is a class 3 grid.

Grid map:

The below grid shows an example distribution with 3 sample group size.

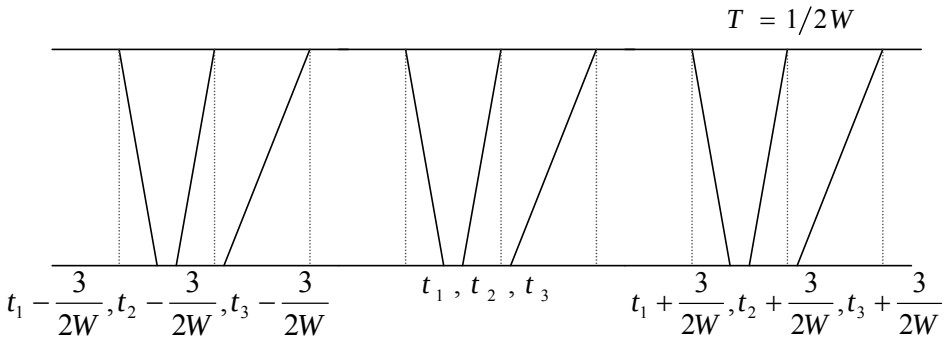

Conditions on distribution:

1-The Average sampling rate should be the Nyquist rate, where the average sampling rate can be related to the number of sample points per unit time if Nyquist sampling were applied.

2-Although in theory, arbitrary amounts of shifts are allowed, in a practical setting the maximum allowable time shift for a given sampling instant should not be larger than the Nyquist sampling period.

3-When a sampling instant is shifted to right or left, the neighboring point should be shifted such that no crossover is occurring. If a crossover occurs, the corresponding time instants will adjust themselves to indicate this, however in causal systems the crossover is physically impossible and should be avoided. For only noncausal systems a cross over can be realized, and can also be incorporated to the simulations.

Expression of the distribution:

The sample points are divided into groups of N and the groups have a recurrent period of $N/2W$, where W is the Nyquist frequency, which is also the upper bound of the signal bandwidth. In the base period the sample points are denoted by $t_p, p = 1,2,...,N$. Hence the complete set of sample points are written as $\tau_{pm} = t_p + mN/2W$ with $m = ...-1,0,1,....$. For this distribution, the following theorem is valid:

Theorem 2.3 [Yen 3]

A bandwidth limited (to W hz) continuous signal is uniquely defined by its samples at a set of recurrent sample points $t = \tau_{pm} = t_p + mN/2W$, $p = 1,2,...,N$, $m = ...-1,0,1,....$

The reconstruction is given by:

$$f(t) = \sum_{m=-\infty}^{\infty} \sum_{p=1}^{N} f(\tau_{pm}) \Psi_{pm}(t) \tag{2.5}$$

Where the interpolation function is defined as:

$$\Psi_{pm}(t) = \frac{\prod_{q=1}^{N} \sin(\frac{2\pi W}{N}(t - t_q))}{\prod_{\substack{q=1 \\ q \neq p}}^{N} \sin(\frac{2\pi W}{N}(t_p - t_q))} \frac{(-1)^{mN}}{\frac{2\pi W}{N}(t - t_p - \frac{mN}{2W})} \tag{2.6}$$

2.1.4 Arbitrary nonuniform samples, ANS, (Yen 4)

Definition of sampling strategy:

Also called as the " time-limited " signals, those bandlimited signals have the property that when sampled uniformly, all the sample values outside a time interval T vanish. (Strictly speaking, a signal can only approximately be both band and time limited at the same time, due to uncertainty principle) This means that the signal can be specified by 2WT sample points, where W is the signal bandwidth. When one does not wish to specify the time interval explicitly, the 2WT sample points can still be used to define a "minimum energy " signal uniquely according to the following theorem.

Grid map:

No structure is proposed for the sampling point distribution. All the points are at arbitrary locations in their boundary cells; hence this is a completely random sampling instant distribution. No specific grid exists.

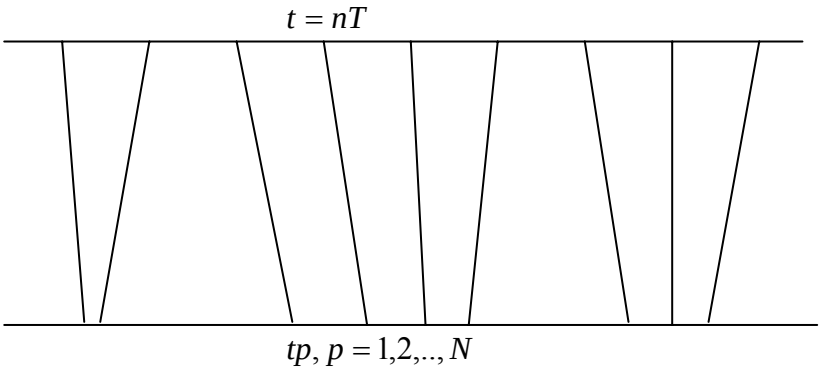

Conditions on distribution:

The minimum energy signal condition should be judged correctly. Also the time and band limited signal condition should be carefully applied. The sample point distributions are arbitrary, however within two conditions; the average sampling rate is still Nyquist rate and no crossovers are allowed.

Definition of the Distribution:

Completely random distribution, sampled at the average Nyquist rate, no crossovers allowed.

Theorem 2.4 [Yen 4]:

If the sample values at a finite set of arbitrarily distributed sample points $t = \tau_p$, $p = 1,2,..., N$ are given, a signal $f(t)$ with no frequency components above W hertz is defined uniquely under the condition that the signal is a minimum energy signal (i.e. $\int_{-\infty}^{\infty} f(t)^2 dt$ is a minimum).

The reconstruction of the signal is;

$$f(t) = \sum_{p=1}^{N} f(\tau_p)\Psi_p(t) \tag{2.7}$$

Where the interpolation function is defined as:

$$\Psi_p(t) = \sum_{q=1}^{N} a_{qp} \frac{\sin(2\pi W(t-\tau_q))}{2\pi W(t-\tau_q)} \tag{2.8}$$

And the coefficients a_{qp} are obtained as the coefficients of the inverse of a matrix, whose (the normal matrix) elements are

$$\frac{\sin(2\pi W(\tau_p - \tau_q))}{2\pi W(\tau_p - \tau_q)} \tag{2.9}$$

$p, q = 1,2,.... N$.

2.2 Performance simulation results

The presented algorithms of Yen are implemented with software. And this section shows the corresponding results obtained from simulations. In this chapter 2, the focus of the simulations will be on the interpolation accuracy. The interpolation accuracy will be tested for two points of views. The first includes the accuracy with respect to the signal type, and the second includes the accuracy with respect to the sample point distributions.

To test the first point of view, different signal types are applied to the interpolators. The signal types are the followings: a practically time and band limited signal, a chirp signal and a truncated cosine signal. The time and band limited signal is applied because this type of signals finds a great variety of applications. Hence the performance against such signals is important to know. The chirp signal is applied to test the performance against a nonbandlimited signal. And the truncated cosine is applied to test the performance of the interpolator for a signal that becomes nonbandlimited when processed by finite length systems.

Time and band limited signal is generated according to the following procedure. A random signal is generated and convolved with a lowpass filter, which is designed with a Kaiser type window. Cut off frequency of the filter is set to fit the band limit of the interpolators. The beta parameter of the window is adjusted so that the resulting signal has at least 60 dB attenuation before the Nyquist frequency. Finally, the resulting signal is normalized with its standard deviation so that the final time and bandlimited signal has unity variance. Normalization is applied with every signal type. The chirp signal is generated to begin with the lowest frequency being 10 Hz and linearly approaching to a max frequency that is below the Nyquist frequency. And finally the truncated cosine signal is generated as a combination of a finite number of sinusoidal signal each having a frequency less than the Nyquist rate. The signal has jumping end points.

To test the second point of view, the interpolators are applied a fixed time and bandwidth limited signal with different sample point distribution grids. Therefore the effect of the grid on the interpolation accuracy is observed.

The first group of tests will be applied along the following definition. A signal type is selected and an instance of it is generated. A nonuniform sampling grid is defined and the corresponding uniform and nonuniform samples are acquired from the oversampled signal. The nonuniform samples are input to each interpolator and outputs of the interpolators are obtained. The error of the interpolation is measured as the difference between the uniform samples and the interpolated samples for each type of interpolator, respectively. To find a more reliable value of this error, the test is applied for a number of times and the results are averaged out.

The second group of tests will be applied along the following definition. Throughout the tests, a fixed signal will be applied and only the sampling grid will be changed. The sampling grids will be changed in two ways. In the first set of changes, the whole grid will be regenerated with the same sample point deviation variance, σ^2. While in the second set of changes, the same grid of samples will be applied, each time with a varying deviation amount, characterized by σ^2, again.

Throughout the tests, the length of the corresponding signals will be stated explicitly, for each type of test whenever required. Also in the tests short names of the algorithms will be used as the followings: finite number of nonuniform sampling (Yen 1) as FNS, semi infinite nonuniform sampling (Yen 2) as SINS, recurrent nonuniform sampling (Yen3) as RNS and arbitrary nonuniform points (Yen 4) as ANS.

Note: due to the fact that SINS algorithm uses a very constrained sample point distribution, although its performance showed reasonably good, it won't be added to the overall tests.

A-Simulation results for accuracy with respect to the signal type

A1-Time and band limited signal input

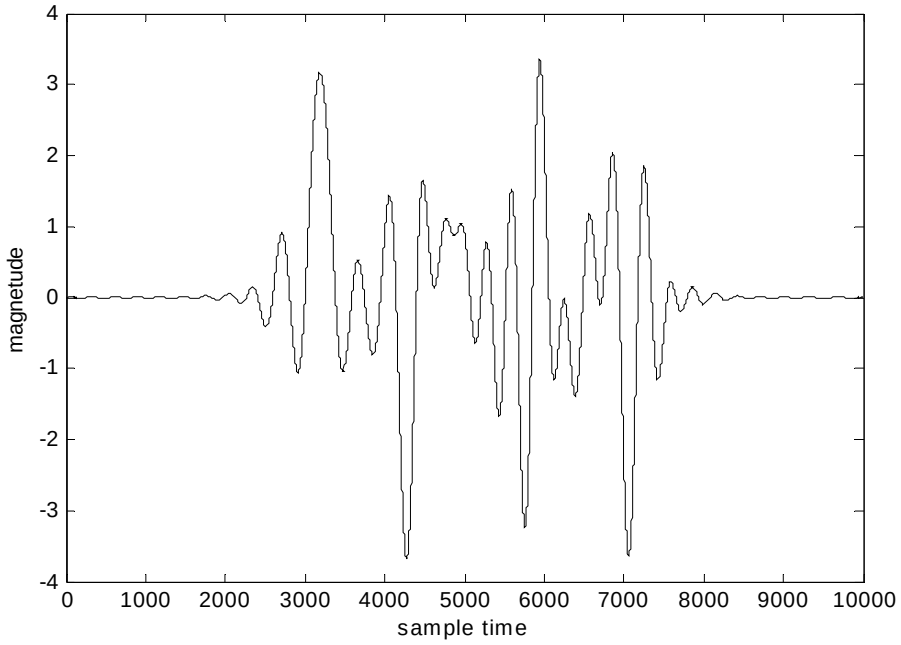

Figure 2.1: Time and band limited input signal

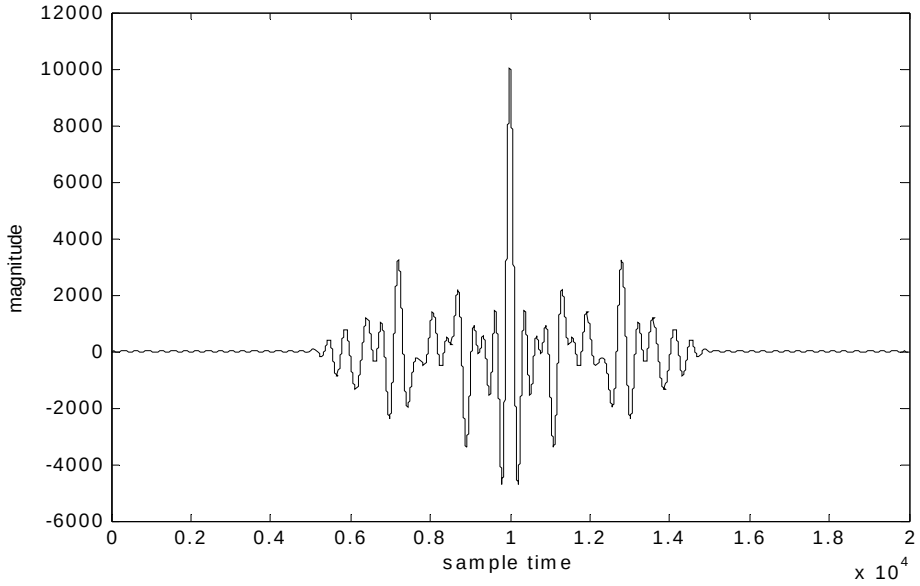

Figure2.2: Autocorrelation of the signal in figure 2.1

Figures 2.1 and 2.2 shows the plots of an instance of the oversampled signal and the autocorrelation sequence of that signal. It is an instance, because at each trial a different signal is applied to smooth the experiment result, however, with the same characteristics. (i.e. same mean, variance and norm)

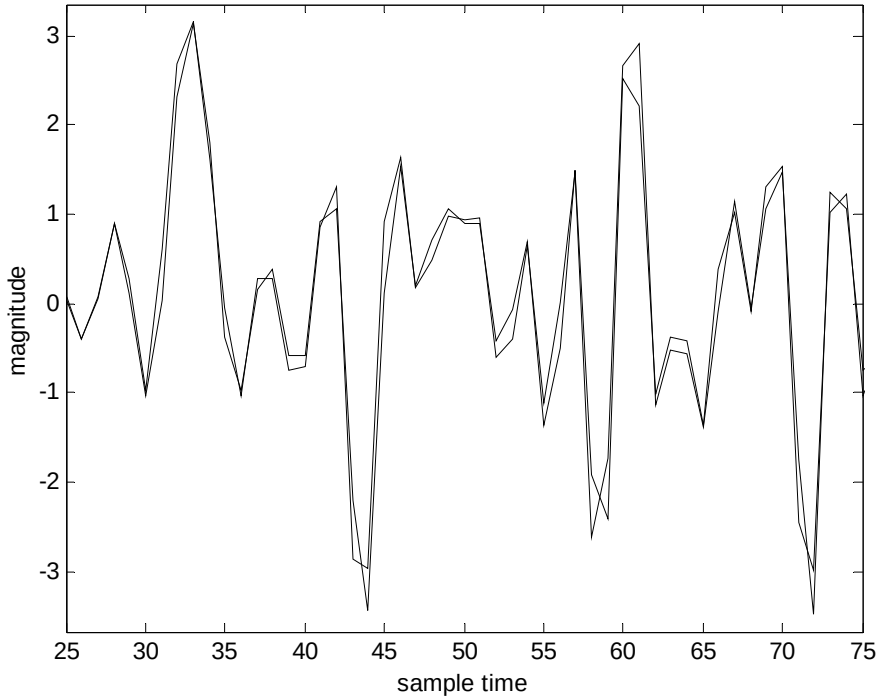

Figure 2.3: Uniform and nonuniform samples of time and bandlimited signal plotted together

Figure 2.3 displays the uniform and nonuniform samples plotted together. Both of them are plotted with same line type, this way the difference between uniform and nonuniform samples can be understood better. The concern of the figure is the difference between the samples, not the actual signals. Looking at the figure more carefully, the discrepancies are easily observed. One thing should be noted that, the actual positioning of the nonuniform samples are not the ones that are plotted as in the figure. The actual positions are between the uniform samples, which are not suitable to plot. Figure 2.4 displays the dft of the uniform samples. By definition the frequency content of the uniform samples is attenuated by at least 60 dB prior to the Nyquist frequency. The frequency content of the nonuniform samples is not shown because dft

inherently relies on uniform sampling. It should be clear that the frequency contents of the two signals, the uniform and the nonuniform, are the same, for they belong to the same signal. However when uniform dft of the nonuniform samples is calculated, the result will be drastically different from those of the uniforms. Hence, it is not plotted.

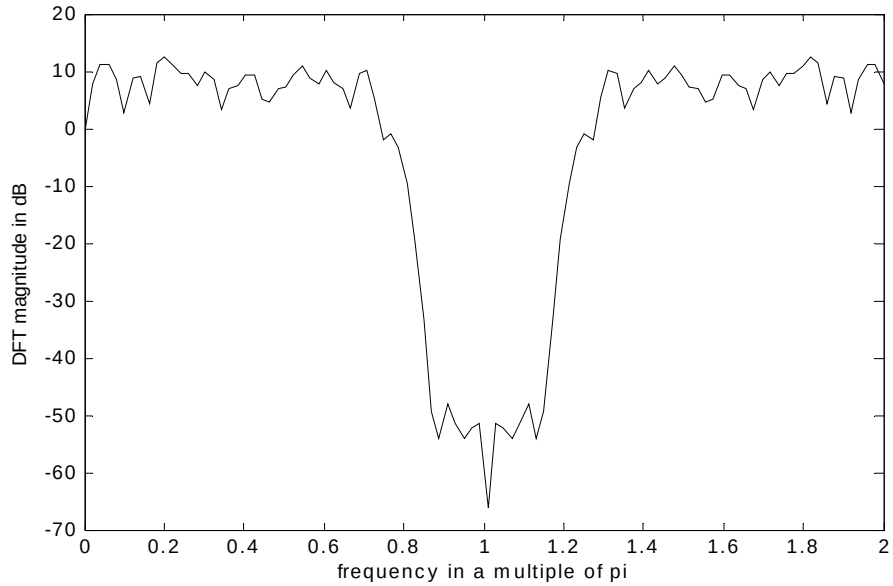

Figure 2.4: Frequency plot of uniform samples obtained from time and band limited signal.

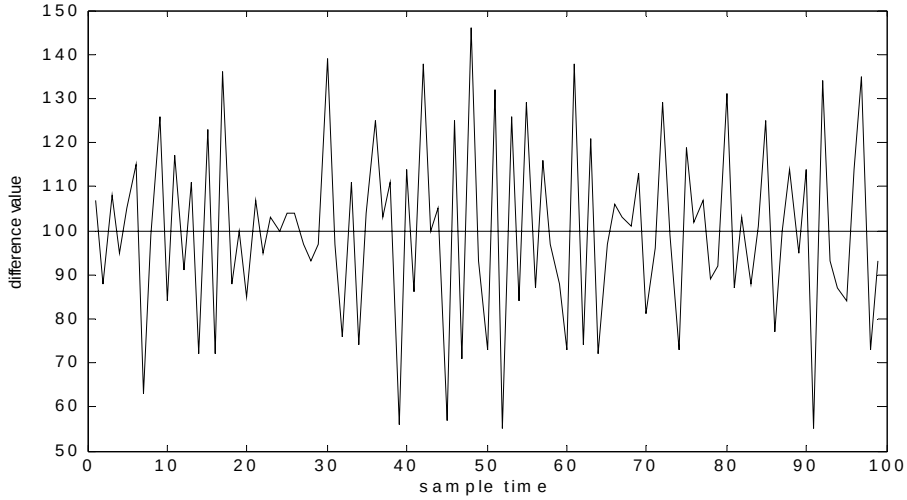

Figure 2.5: Sampling instants nonuniformity plot

Figure 2.5 displays a very useful visualization of the amount of nonuniformity present in the respective nonuniform sample distribution. The difference of the sampling instants for each consecutive sampling point are plotted. And the normal uniform distance is referenced as the bar across the sample index. In a rough estimate, the amount of nonuniformity is directly proportional to the variance of the distribution. So by looking at the difference plots we can visualize the amount of nonuniformity that was present in the distribution.

Figure 2.6 shows the interpolation results of the given signal instance. As can clearly be seen, all the interpolators seem to produce the same outputs, which is also identical to the uniform samples. In fact, the seemingly same outputs may differ in a number of orders from each other. This difference can best be visualized from a log magnitude error plot, which is plotted in figure 2.7

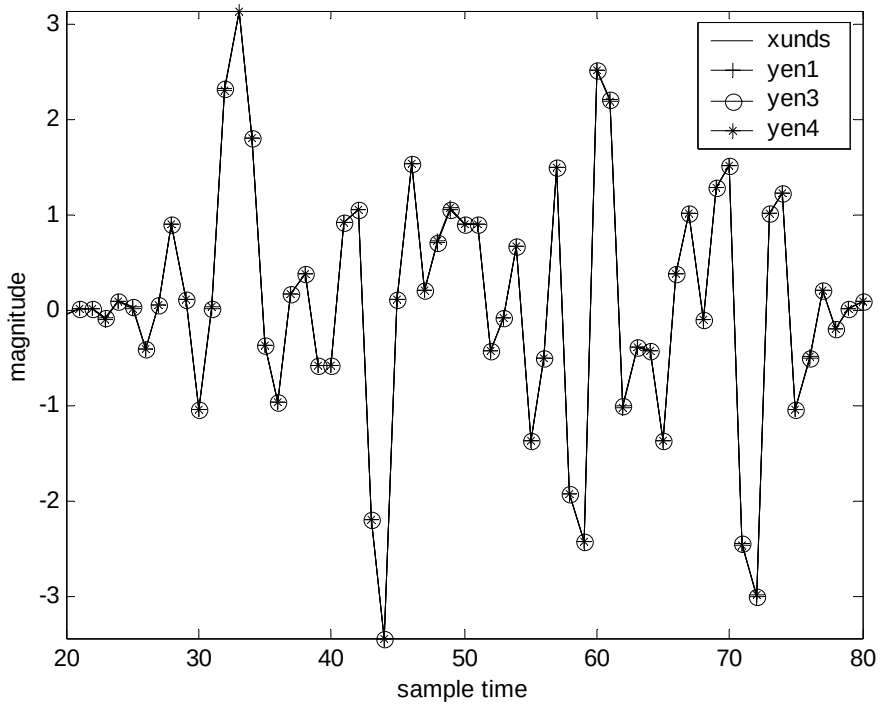

Figure 2.6: Interpolation outputs, for time and band limited signal

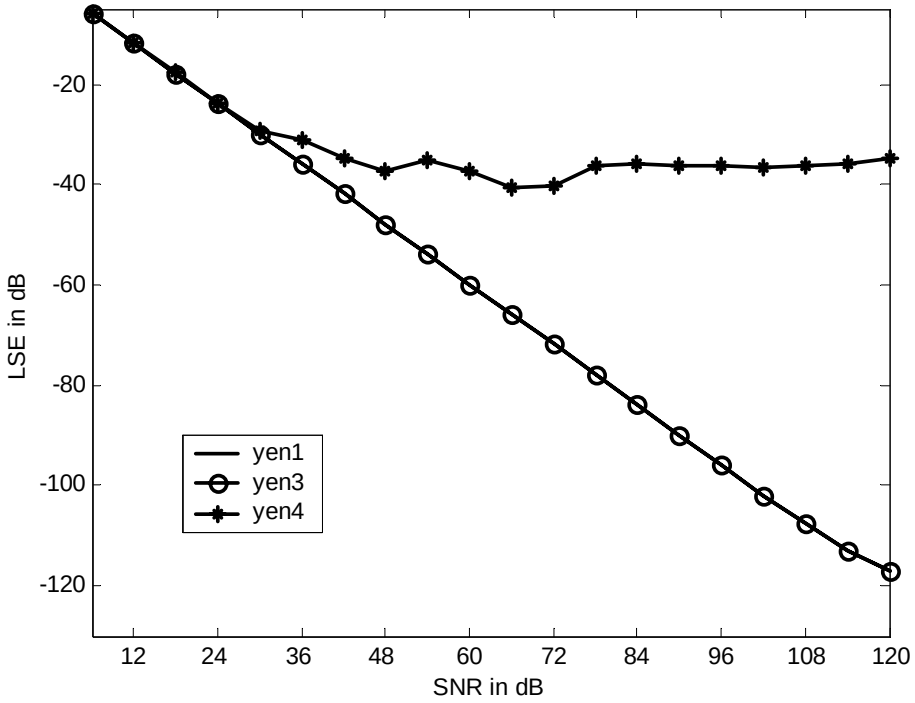

Figure 2.7: LSE for time and band limited signal interpolation

Figure 2.7 shows the corresponding errors of interpolation for Yen's classical algorithms. It is observed that the algorithms Yen 1 and Yen 3 display an almost equivalent performance, Yen 3 being slightly better, not observable from the figure due to scaling. And it is apparent that, Yen 4 falls far behind of the Yen 3 and 1, representing a constant interpolation error floor around –35 dB for increasing SNR after 36 dB. Whereas Yen 1 and 3 shows as much as –120 dB accuracy for this simulation.

A2-Chirp signal input

The figures 2.8 and 2.9 show a sample chirp signal and its correlation sequence. The chirp signal has a beginning frequency of 10 Hz and a final frequency of $2Fsam/5$ Hz, where $Fsam$ is the corresponding sampling frequency used in the tests.

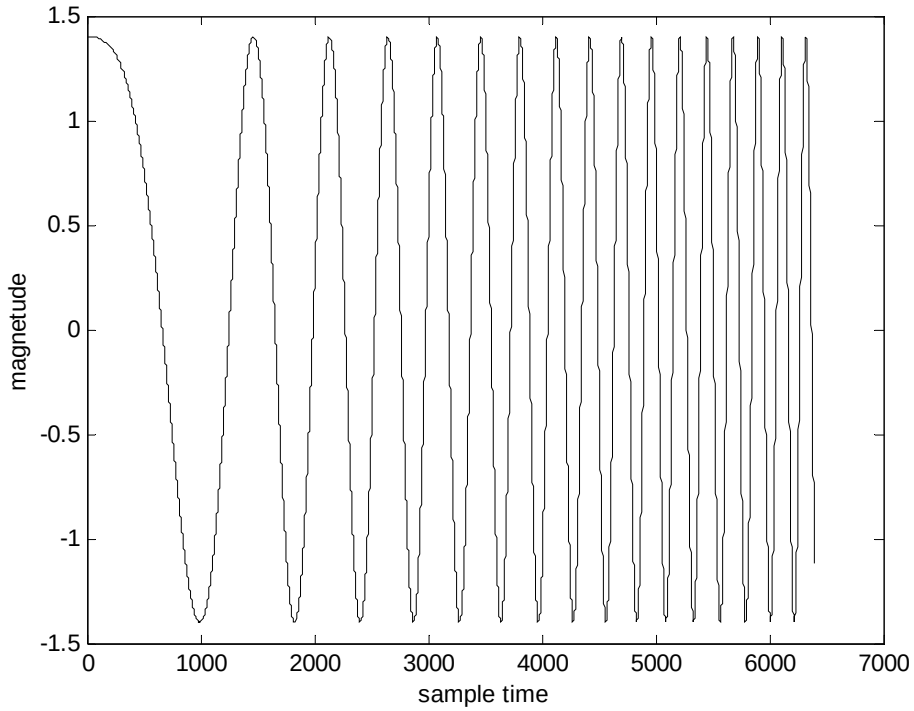

Figure 2.8: The chirp signal to be applied to the interpolator

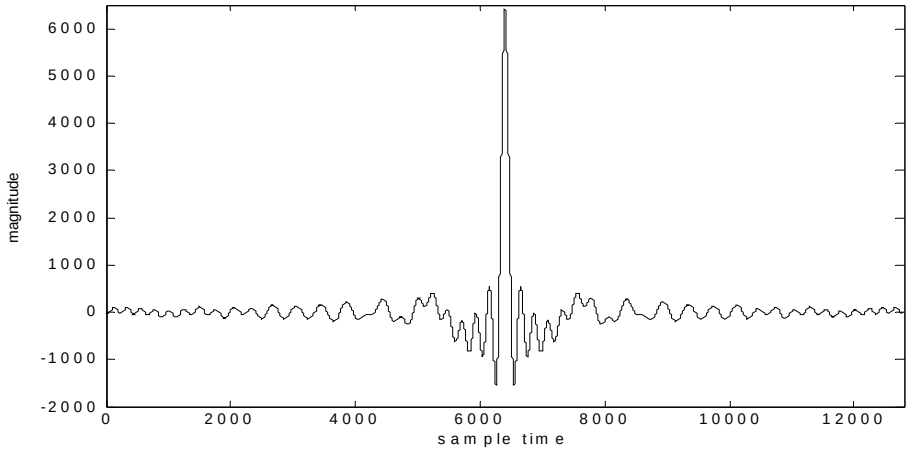

Figure2.9: Autocorrelation of oversampled chirp

Figure 2.10 shows the corresponding uniform and nonuniform samples plotted as in fig 2.3. This time the differences are more difficult to see and they tend to occur to the end of the signal where frequency approaches the Nyquist limit.

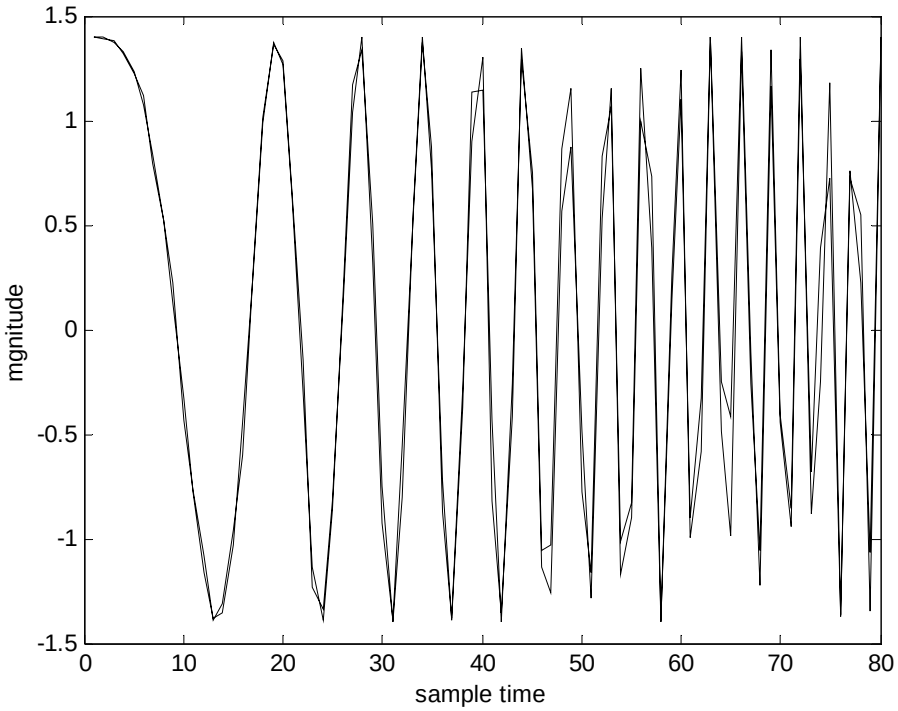

Figure 2.10: Uniform and nonuniform samples of chirp signal plotted.

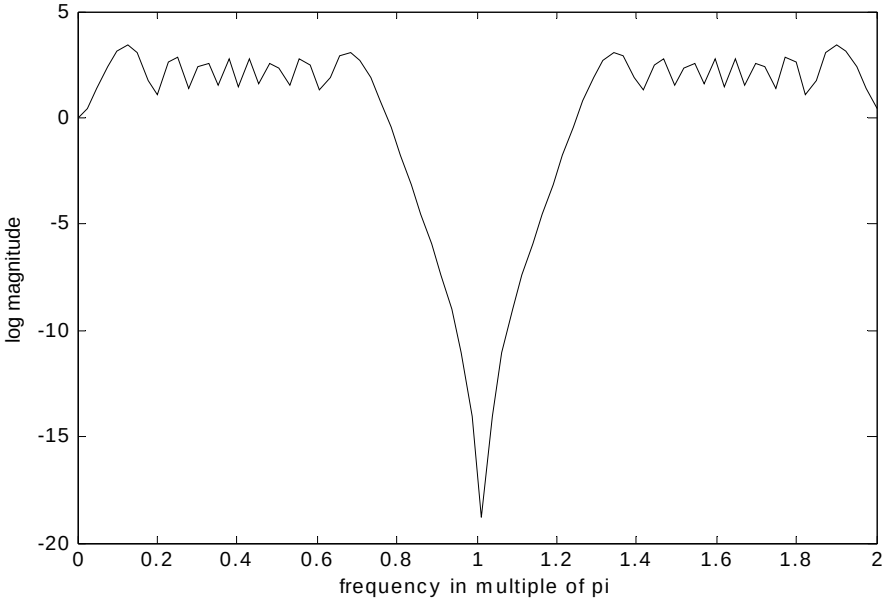

Figure 2.11: Frequency spectrum of uniform samples

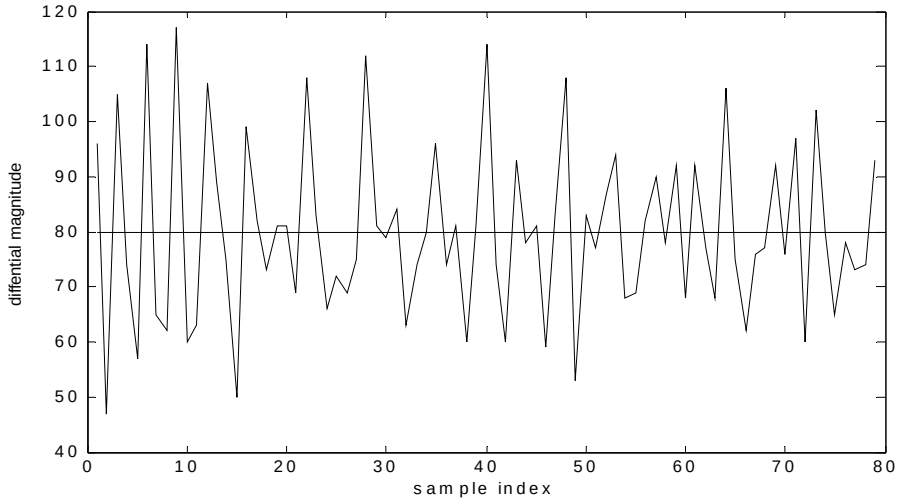

Figure 2.12: Sampling instants nonuniformity plot

Figure 2.11 shows the corresponding spectrum of uniform samples at a signal length of 80 samples. The spectrum of the resulting uniform samples can be seen to have considerable energy to the Nyquist frequency. This is the main reason of having more interpolation error for the simulation of chirp signal input. And the figure 2.12 shows the distribution characteristics of the nonuniform sampling instants. This grid was used to obtain the nonuniform samples with a length of 80. Whereas the following figures shows the corresponding interpolations, and the errors associated with them.

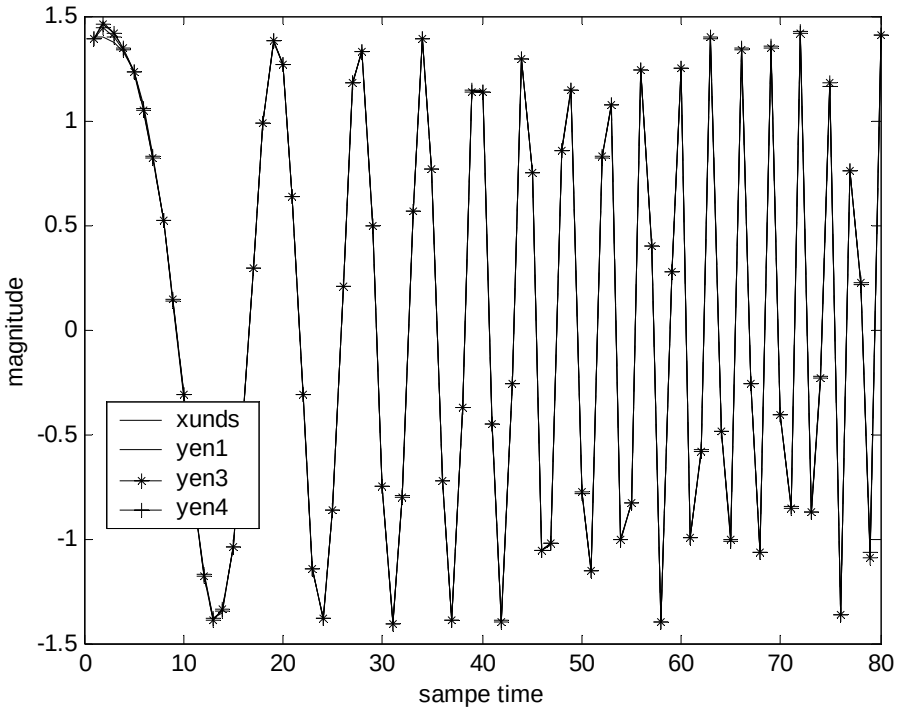

Figure 2.13: Results of chirp signal interpolations

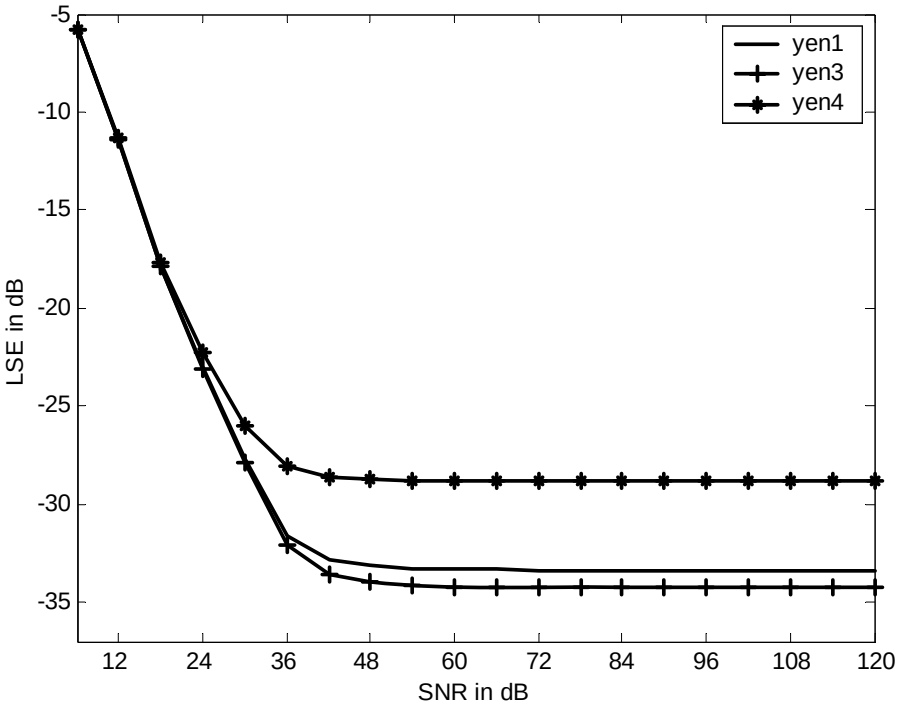

Figure 2.14: LSE errors of chirp interpolation for increasing signal length

Looking at the figure 2.14, it can be seen that performances of the interpolators for this type of signal is quite low. This fact is understandable because the signal is nonbandlimited, as can be seen from the dft plot of it. Again Yen 1 and 3 shows close performances, with Yen 3 having the least error. In contrast to bandlimited interpolation results, chirp signal interpolation stops responding to increasing SNR after a limit value of the error is reached. Taken from another point of view, the error floors of all interpolators are much higher than the bandlimited interpolation. From the figure it is again observed that Yen 4 represents the least accurate result.

A3-Truncated cosine input

The last part of the, performance with respect to signal type, simulations show the performance for a truncated cosine signal. This signal is nonbandlimited due to the truncation at the ends. However its content seems bandlimited. Figure 2.16 shows the auto correlation of the sinusoids revealing the fact that signal is a periodic wave with high degree of correlation.

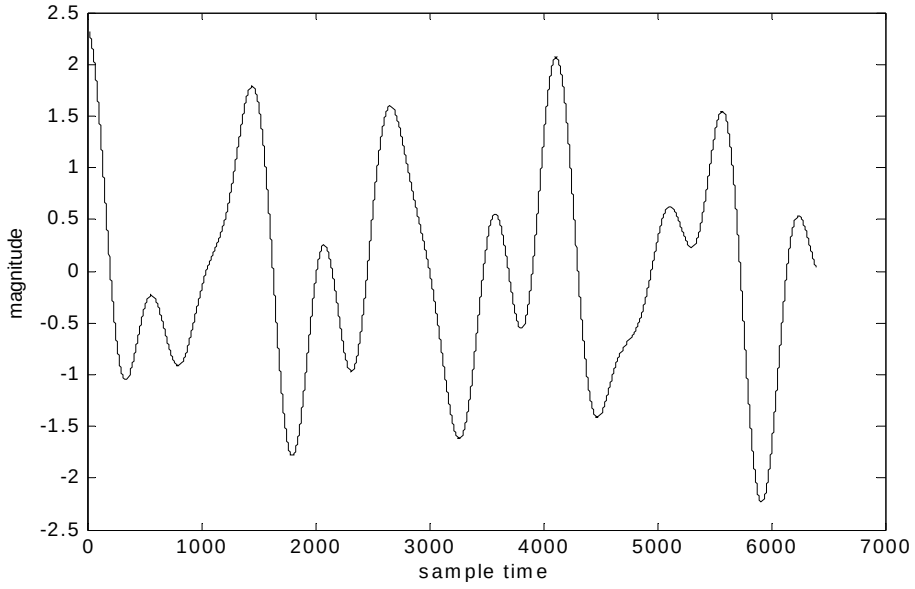

Figure 2.15: Truncated cosine signal

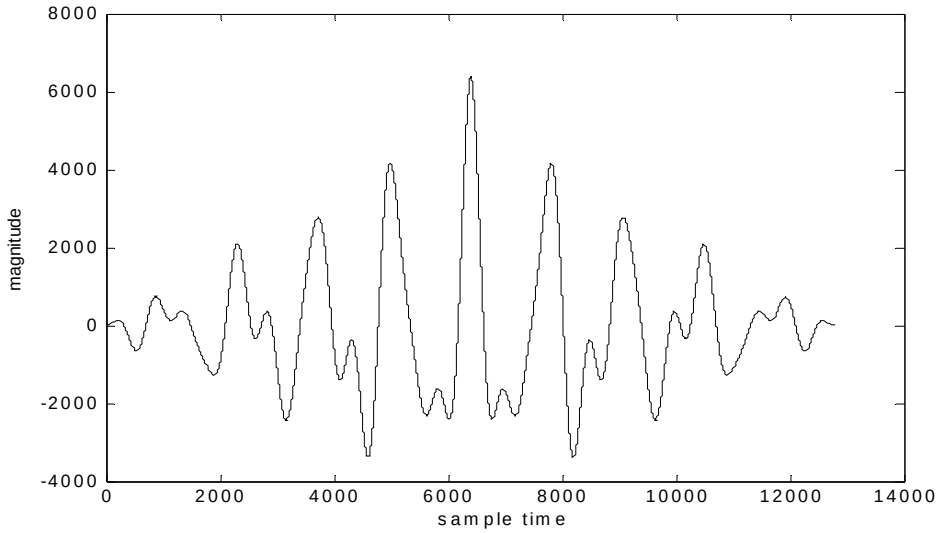

Figure 2.16: Autocorrelation sequence of input

Figure 2.17 shows the uniform and nonuniform samples. Due to the differences, the plot becomes scratchier. The amount of the scratch represents the amount of nonuniformity. Though it is not clear, nonuniformity is same with the former tests

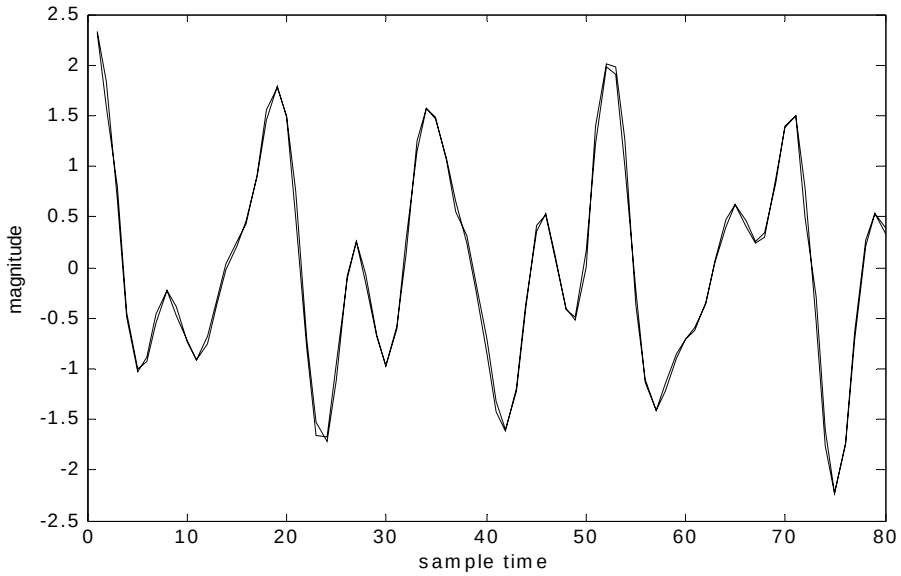

Figure 2.17: Uniform and nonuniform samples of truncated cosine signal

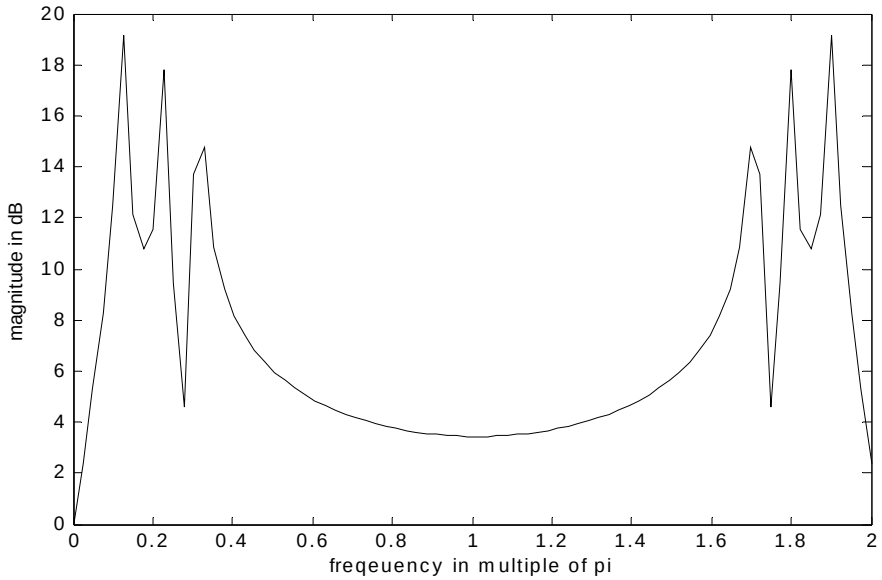

Figure 2.18: Frequency plot of uniform truncated cosine signal samples

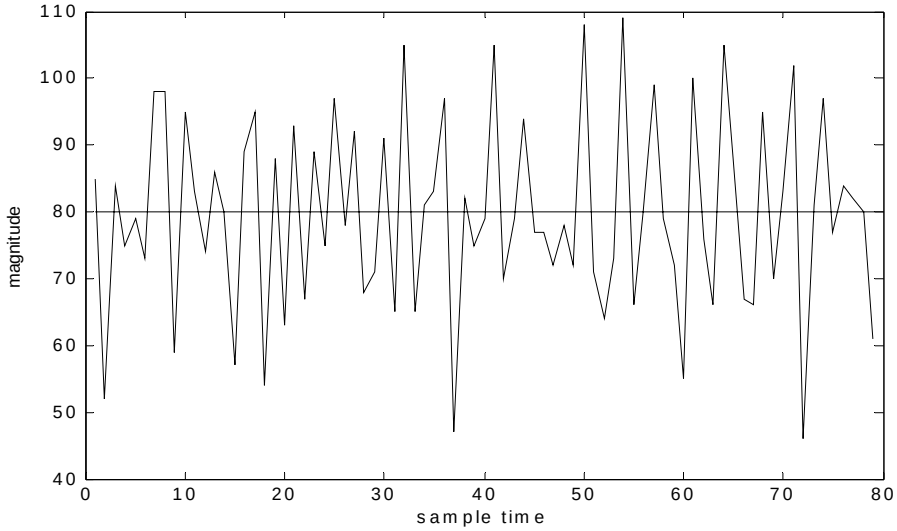

Figure 2.19: Sampling instant nonuniformity plot

Figure 2.18 shows the dft of the uniform samples, this dft exhibits the worst characteristics. There are line components in it. And it has nonzero value at the Nyquist frequency. The sample point distribution nonuniformity is plotted in figure 2.19.

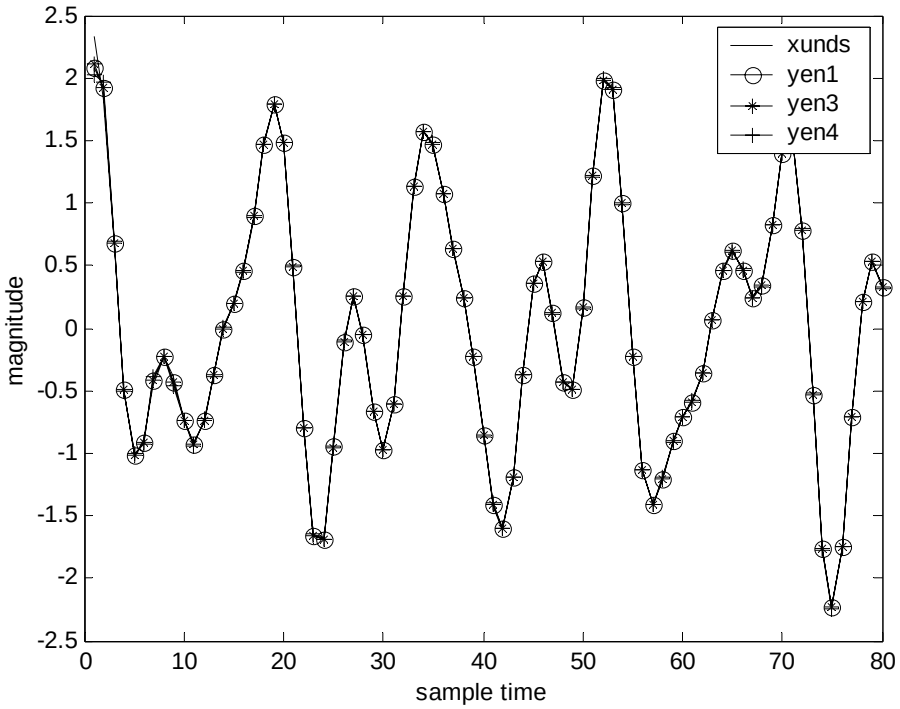

Figure 2.20: Truncated cosine interpolation results

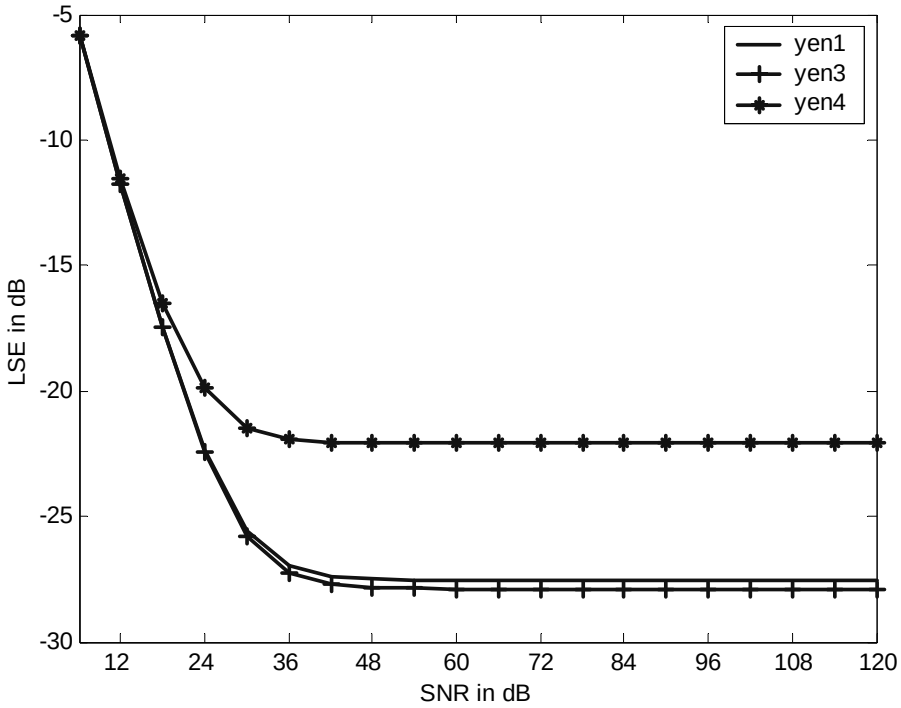

Figure 2.21: LSE of truncated cosine interpolations

The figures 2.20 and 2.21 show the interpolations and the log magnitude LSE errors. It is observed from the figure that the truncated periodic signal interpolation generates the most erroneous result. This can be easily understood from the figure 2.20 where the dft of the uniform samples of the signal shows considerably more energy than the former two cases. Hence the interpolation is less accurate. Also observed from figure 2.21 is that Yen 4 shows the worst interpolator while Yen 3 represents the best interpolator of this part A of the simulations.

B-Simulation results for accuracy with respect to sampling point distribution

In this part B, algorithms will be tested for their interpolation accuracy with respect to a changing sampling grid. The signal used in this test will be the same of that was presented in test A1, A practically time and bandlimited signal. Two types of sample point distribution changes will be analyzed. The first type will be a change of the distribution, preserving the variance. While the second will be the change of variance, that is obtained by multiplying a given fixed set of grid distribution with the appropriate coefficient so that the resulting grid has the required variance. The variance of the distribution is calculated by normal means.

B1-Result of interpolation with respect to different distributions

Figure 2.22 clearly shows two facts. The first is the fact that ANS interpolator performs much worse than the FNS and RNS interpolators, which was already demonstrated in part A. However the second interesting fact is that the dependence on sample point distribution is more dramatic for ANS than the FNS and RNS. In other words, RNS and FNS performances are more robust with respect to sample point distributions.

They show almost the same performance with different distributions, whereas ANS shows a larger error variance. If ANS is used with the same signal conditions, as large as 20dB accuracy may be lost (between sixth and seventh trials), for only the sample point distribution being different. This is clearly an unexpected and undesired result and should be considered carefully.

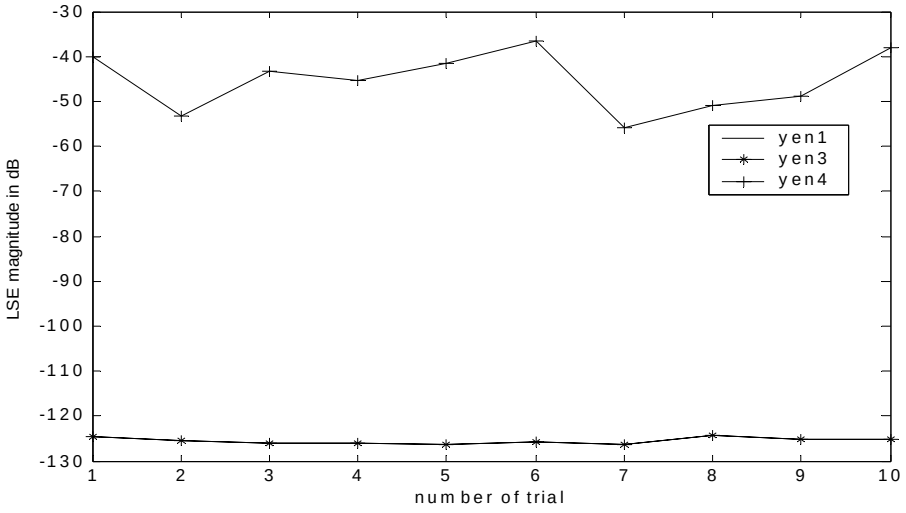

Figure 2.22: LSE of interpolation for 10 different sample distributions

B2- Result of interpolation with respect to distributions variance

Figure 2.23 shows the difference between uniform and nonuniform samples obtained by the maximum variance of distribution. As clear, large deviations exist.

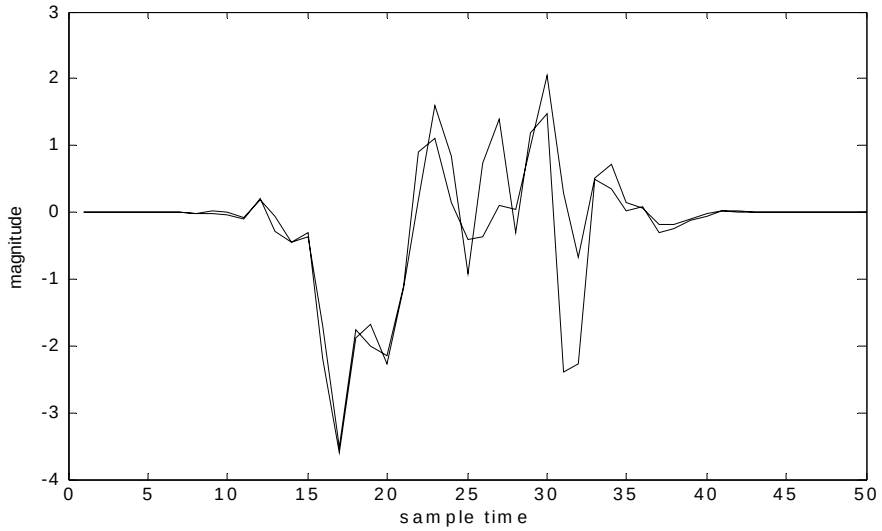

Figure 2.23: Uniform and nonuniform samples obtained from a time and band limited signal with maximum distribution variance

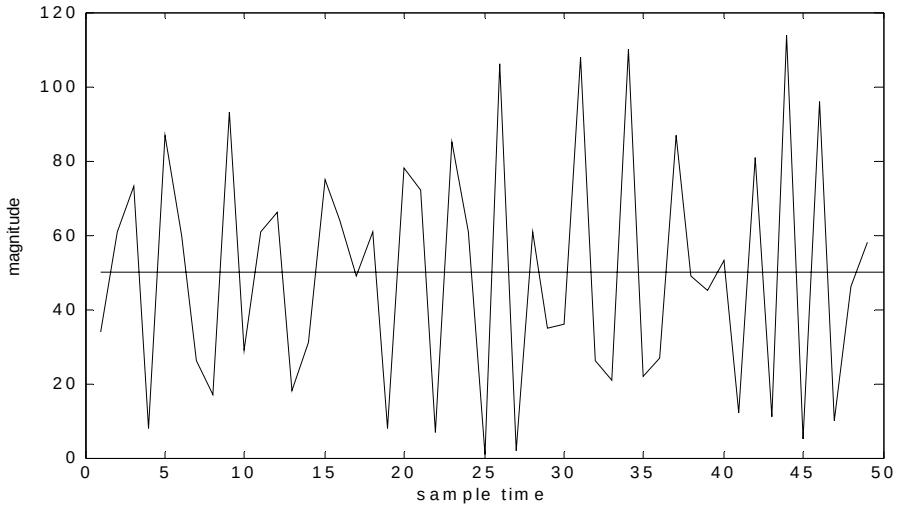

Figure 2.24: Sampling instants nonuniformity plot

Figure 2.24 displays the sample point distribution with a variance of 390. The absolute value of the variance is not relevant, it simply measures the

amount of deviations of sample points from their uniform locations. By looking at figure 2.25 it is observed that the performance of interpolators is at their supreme when the variance is at a minimum, the points are closest to their uniform locations. As the variance is increased, the sample points get far away from the uniform locations. The effect of this is seen by the increase in the LSE magnitude. Again it is observed that ANS has a more dramatic dependence on the variance of the distribution. It is seen that, as indicated by B1, ANS shows strong dependence on sample point distributions. ANS shows an almost 30dB increase in error when the variance makes a full span. And it is again verified that RNS and FNS show little, at most 10 dB, increment in LSE for a full span of distribution variance. What is meant by a variance span is the following. As the points move away from their uniform locations, they tend to leak to the next samples uniform cell. The cell can be described as the interval of sample time, centered at the uniform sample location. Span is a value of variance, upon which most majority of sample points will drift to their neighboring sample cells. And samples make crossovers. The actual variance cannot be increased more, and error tends to become flat, as clearly observed to the end of the figure.

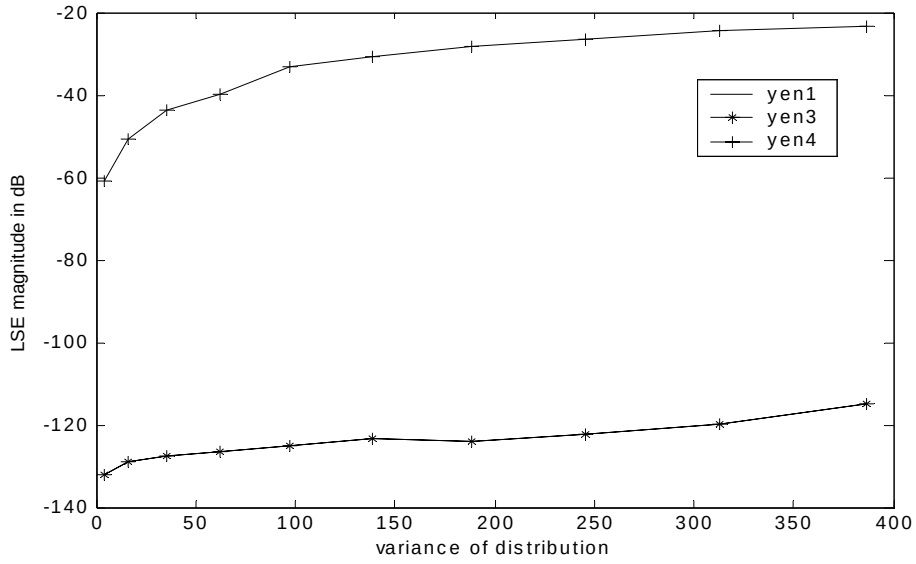

Figure 2.25: LSE with respect to distribution variance

B.3 Missing sample problem simulation

Missing sample problem is encountered in a number of occasions. Therefore a look at the performance of RNS, the best performing interpolator, under such a condition will be beneficial. Figure 2.26 shows a missing sample grid with at least one and at most two samples being missed. This is clearly seen from the middle portion of the grids. The bottom part of the figure shows two sets of sample trains. The larger sample train corresponds to the resulting nonuniform sampling grid positions whereas the shorter sequence shows the Nyquist rate uniform sampling grid positions. The middle portion of the larger sample train shows the missing sample part. Also it should be noted that to the end of the sampling grid, an oversampling condition is observed. Hence the average number of samples is preserved. However, the position at which those oversamples are taken has little effect on the interpolation, which means that they can be discarded without introducing considerable error. Figure 2.27 shows the missing sample problem with a miss of three samples.

The signal that is used is a practically time and bandwidth limited one. Finally, the figures 2.28 and 2.29 show the corresponding interpolations. As apparent from the figures, a miss of two samples is affordable with an error of approximately –50 dB, whereas a miss of three or more samples is not affordable, yielding an error of –20 dB for the corresponding simulation.

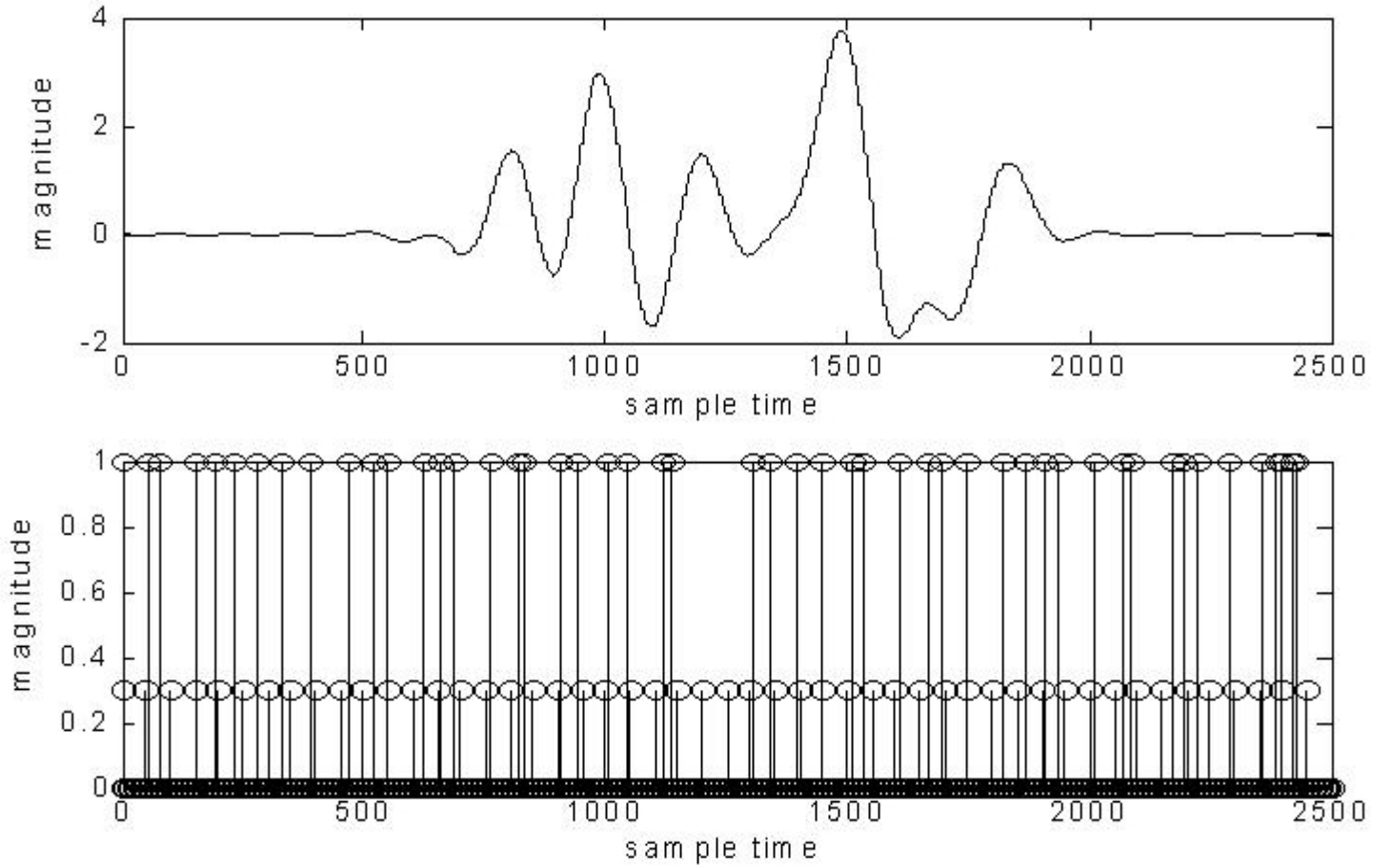

Figure 2.26: Missing sample problem demonstration. The bottom figure shows nonuniform (with value 1), and uniform (value 0.3) grids. At the middle part, at least one sample location is shifted so that no sample is taken. Interpolation lse = -50 dB

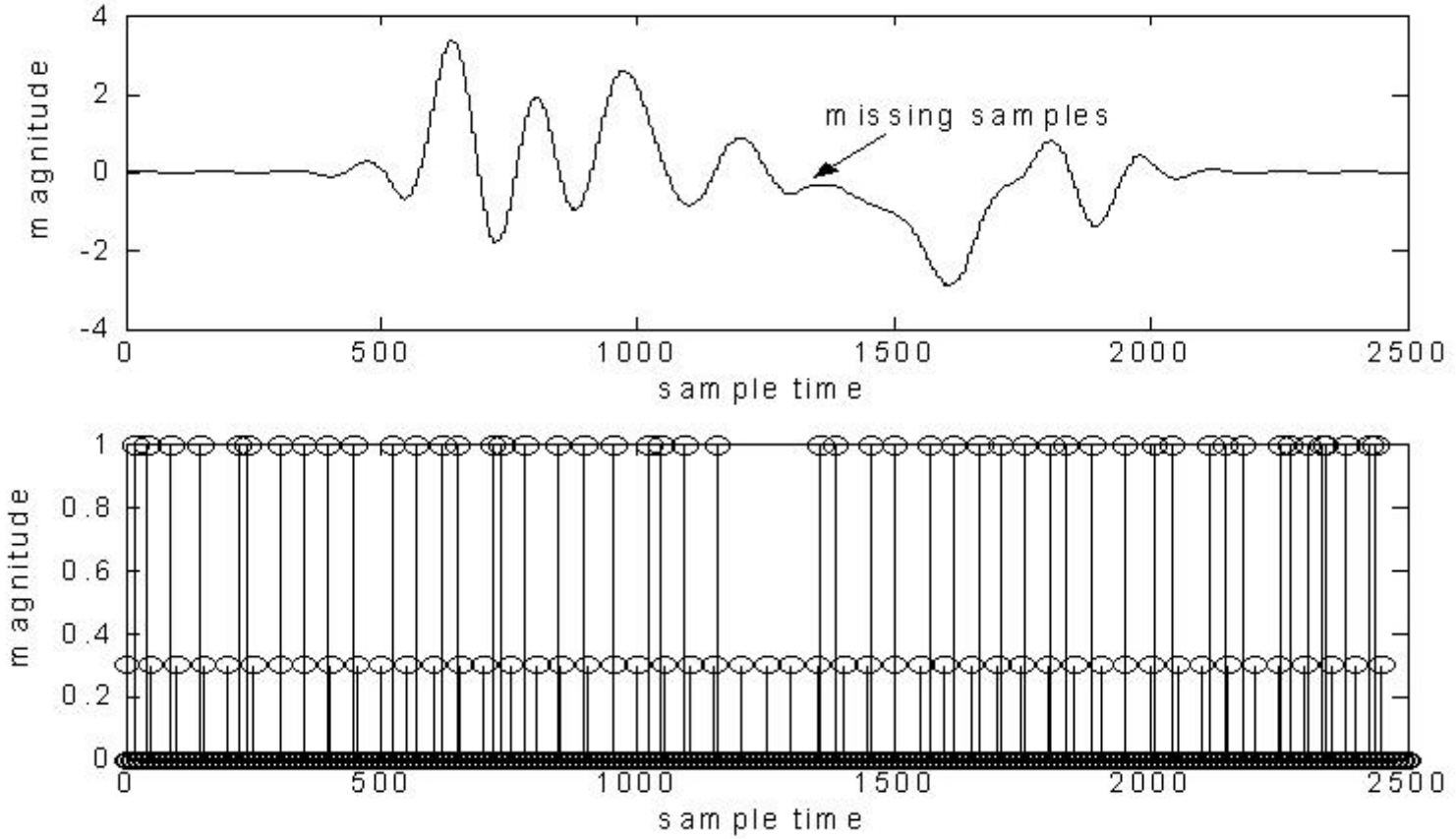

Figure 2.27: Missing sample demonstration with a larger gap. At the middle part, three samples seem to loose their instants. Looking to the end of the sampling grid, an oversampling condition is observed. Interpolation mse = -20dB

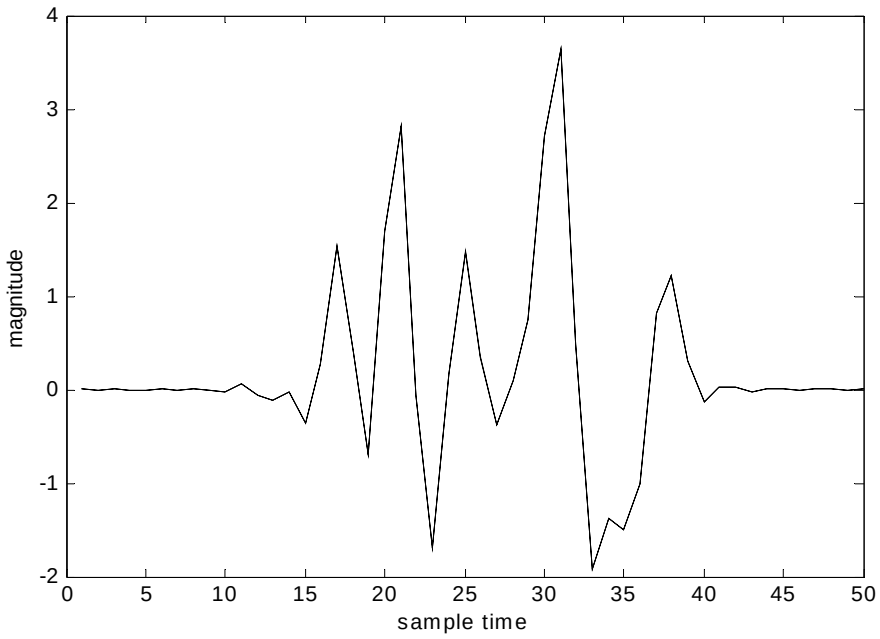

Figure 2.28: Two missing sample interpolation, plotted on uniform samples

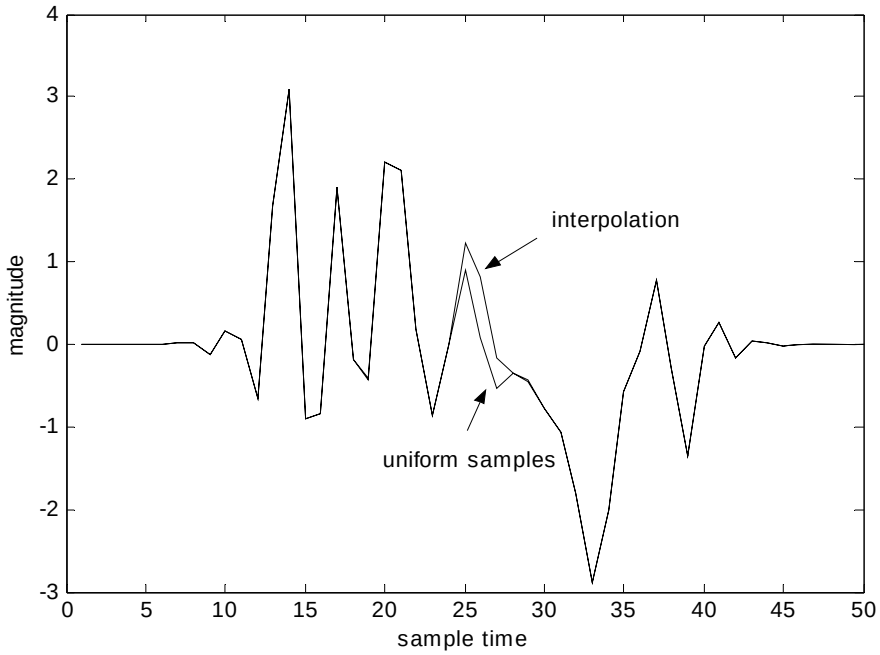

Figure 2.29: Three missing sample interpolation, plotted on uniform samples

CHAPTER 3

EFFICIENT IMPLEMENTATIONS

Chapter 2 demonstrated four classical, well known, algorithms for the reconstruction of signals from their nonuniform samples. The aim of the chapter was on the interpolation accuracy of the respective algorithms. This chapter will focus on the implementation efficiency of nonuniform interpolators. And, an efficient implementation based on filter bank approach will be explicitly shown for the recursive nonuniform sampling algorithm.

3.1. Filter bank implementation for computational efficiency

There exist a great deal of literature about converting signal processing algorithms into efficient implementations. The most well known result is the fact that whenever a given signal-processing algorithm can be put in a form that is equivalent to a linear filtering, then the greatest efficiency is said to be achieved. The reason is that, linear filtering, the most well known signal processing algorithm, can be implemented based on the well known FFT algorithms. For this reason, the first thing to do when increasing the computational efficiency of an algorithm is to find an equivalent filtering structure that implements the given algorithm. Unfortunately it is not always possible to find an equivalent linear filtering structure for every algorithm.

3.1.1 Filter bank implementation method

What follows is an efficient implementation of one of the most respected nonuniform reconstruction algorithms. Yen algorithm 3 was based on the recurrent nonuniform sampling grid. The accuracy performance of the algorithm was so impressive that it could be very useful if an efficient implementation could also be found. Oppenheim and Eldar [18] have demonstrated an efficient implementation of recurrent nonuniform sampling algorithm.

[18] uses an identity called the "Interpolation identity" to convert an analog filter bank implementation into a discrete one. By this way many advantages over analog implementation are obtained. The most important being the versatility of digital signal processing hardware that can implement multirate processing algorithms with the most efficiency.

The essence of the procedure has four steps to be applied. First an algorithm that is the main aim is provided. Nonuniform reconstruction algorithm will be the aim in this implementation. The algorithm should be suitable for the application of the interpolation identity. Then by applying certain signal processing manipulations, the reconstruction formula is converted into an analog filter bank structure. The third step is to apply the interpolation identity to the analog filter bank and convert it into the equivalent discrete time filter bank structure. The last thing to do is derivation of the corresponding discrete time channel filters. They are defined by using the interpolation identity as, the sampled versions of the analog channel filters. Hence when the algorithm finishes, the resulting filter bank implementation of the recursive nonuniform reconstruction algorithm is obtained. Interpolation identity is presented in [18]. Here a special case, a single channel equivalent of it, is reproduced. We have a single channel analog interpolator replaced by a single channel discrete time equivalent.

Writing the identity for M=1, where M is the number of channels that identity applies, the following equality is obtained.

$$\widetilde{H}(w) = \frac{1}{T_Q} H\left(\frac{w}{T_Q}\right), \ |w| \le \pi \qquad (3.1)$$

Where, $\widetilde{H}(w)$ is the discrete channel equivalent of the analog channel filter $H(\Omega)$. Hence the impulse response of the corresponding discrete filter will be the following.

$$\widetilde{h}[n] = h(nT_Q) \qquad (3.2)$$

The figure below shows the single channel equivalent of the interpolation identity. Note that since $T = NT_Q$ the signal $x_c(nT)$ is an undersampled version of the signal $x_c(t)$

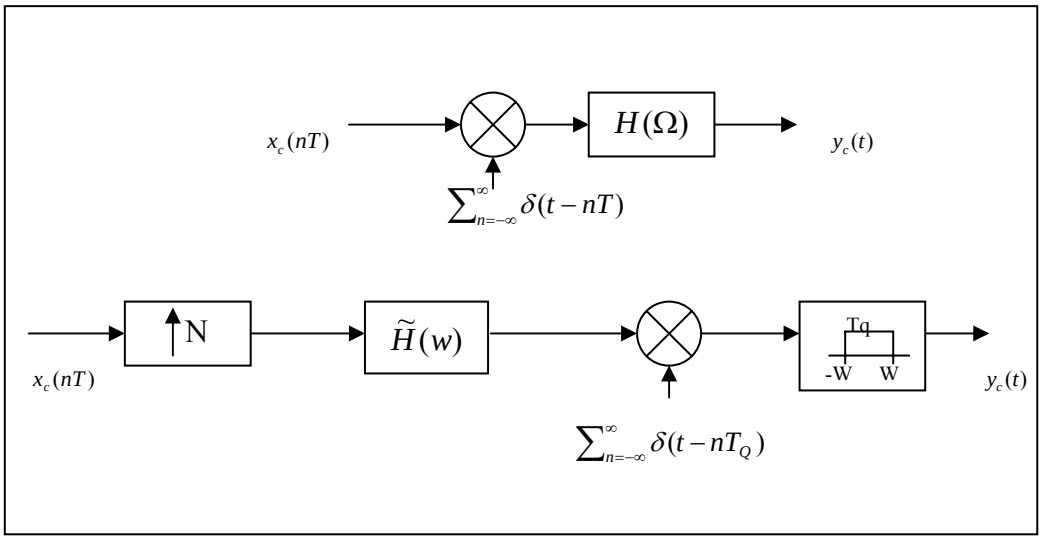

Figure 3.1: Single channel interpolation identity

The upper part of the figure 3.1 shows an analog channel, with analog channel filter denoted by $H(\Omega)$, and the identity converts this analog channel into the equivalent discrete one, with its filter denoted by $\widetilde{H}(w)$. Note the differences in the topologies of the branches.

Filter bank implementation steps of Yen algorithm 3:

Step 1: Recurrent nonuniform sampling and reconstruction revisited.

(Refer to section 2.1.3. for most details) One point to note that the period T_Q used below represents the Nyquist sampling period, which is defined as $1/2W$ in 2.1.3, and the period T is used for NT_Q, the group period.

As shown in section 2.1.3, such a distribution can be shown to have a closed form interpolation formula. [18] reproduces the result as follows:

$$x_c(t) = \sum_{n=-\infty}^{\infty} \sum_{p=0}^{N-1} x_c(nT + t_p) \frac{a_p (-1)^{nN} \prod_{q=0}^{N-1} \sin(\pi(t - t_q)/T)}{\pi(t - nT - t_p)/T} \tag{3.3}$$

where

$$a_p = \frac{1}{\prod_{\substack{q=0 \\ q \neq p}}^{N-1} \sin(\pi(t_p - t_q)/T)} \tag{3.4}$$

Step 2: Derivation of the analog filter bank.

Derivation details can be seen in appendix C. According to the procedures described in appendix C the reconstruction equation (3.3) can be rewritten as a convolution operation**.** Specifically we have

$$f_p(t) = s_p(t) * h_p(t) \tag{3.5}$$

Where the $h_p(t)$, the p[th] analog channel filter impulse is given as

$$h_p(t) = a_p \frac{\prod_{q=0}^{N-1} \sin(\frac{\pi}{T}(t + t_p - t_q))}{\frac{\pi}{T}t} \tag{3.6}$$

and $s_p(t)$ is an impulse train of samples as

$$s_p(t) = \sum_{k=-\infty}^{\infty} x_c(kT + t_p)\delta(t - kT - t_p) \tag{3.7}$$

Now we can express $x_c(t)$ as the below summation

$$x_c(t) = \sum_{p=0}^{N-1} s_p(t) * h_p(t) \tag{3.8}$$

As a result, the continuous signal is represented as the summation of N, linear time invariant convolutions which can be implemented by N channel filtering operations. According to step 2, the resulting analog filter bank can be represented with the following figure.

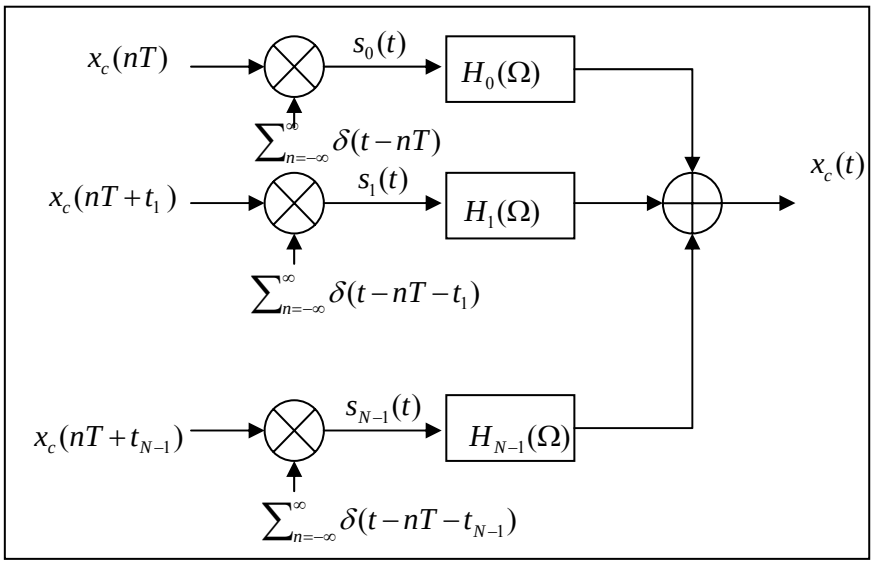

Figure 3.2: Analog filter bank

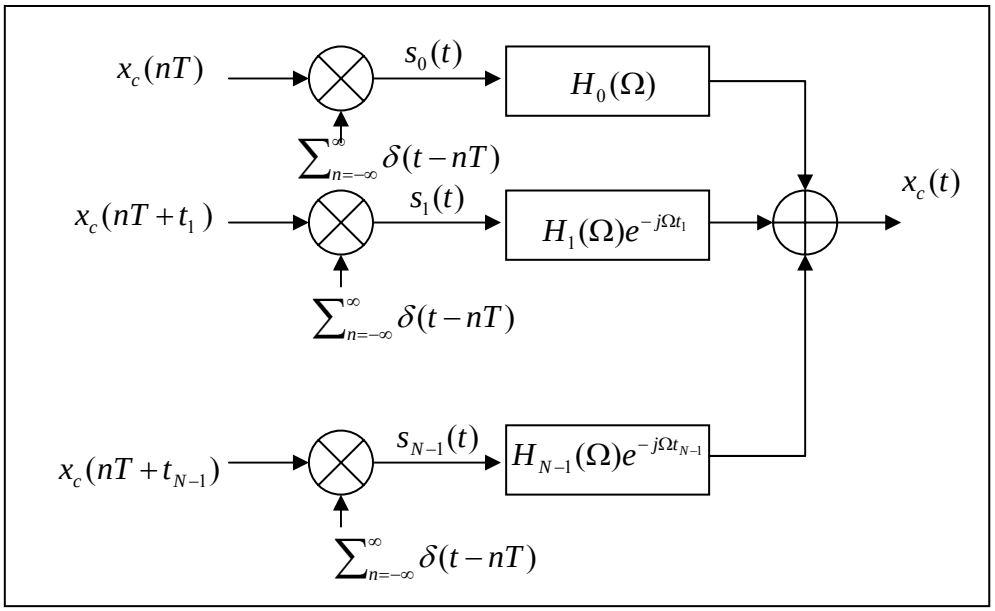

Figure 3.3: Analog filter bank with phases incorporated to filters

Step 3: Determination of the discrete time channel impulse responses.

In step 2, the analog channel impulse response was derived as

$$h_p(t) = a_p \frac{\prod_{q=0}^{N-1} \sin(\frac{\pi}{T}(t + t_p - t_q))}{\frac{\pi}{T}t} \tag{3.9}$$

It was also shown in figure 3.3 that the time shifts of the impulse trains should be incorporated into the filter impulse responses. Therefore the resulting analog channel filter definition (that the discrete system will be derived from) becomes the following:

$$\widetilde{h}_p(t) = h_p(t - t_p) \tag{3.10}$$

and

$$\widetilde{h}_p(t) = a_p \frac{\prod_{q=0}^{N-1} \sin(\frac{\pi}{T}(t - t_q))}{\frac{\pi}{T}(t - t_p)} \tag{3.11}$$

where $\widetilde{h}_p(t)$ represents the analog channel filter impulse response for the p[th] channel. And the corresponding discrete time channel impulse response can be easily obtained by employing the interpolation identity as follows:

$$\widetilde{h}_p[n] = \widetilde{h}_p(nT_Q) \tag{3.12}$$

Then the discrete time channel filters are defined as below.

$$\widetilde{h}_p[n] = a_p \frac{\prod_{q=0}^{N-1} \sin(\frac{\pi}{T}(nT_Q - t_q))}{\frac{\pi}{T}(nT_Q - t_p)} \tag{3.13}$$

Step 4: Conversion to discrete time filter bank

Applying the interpolation identity to each branch in figure 3.3, the corresponding discrete time filter bank is obtained and it's shown as in the figure 3.4.

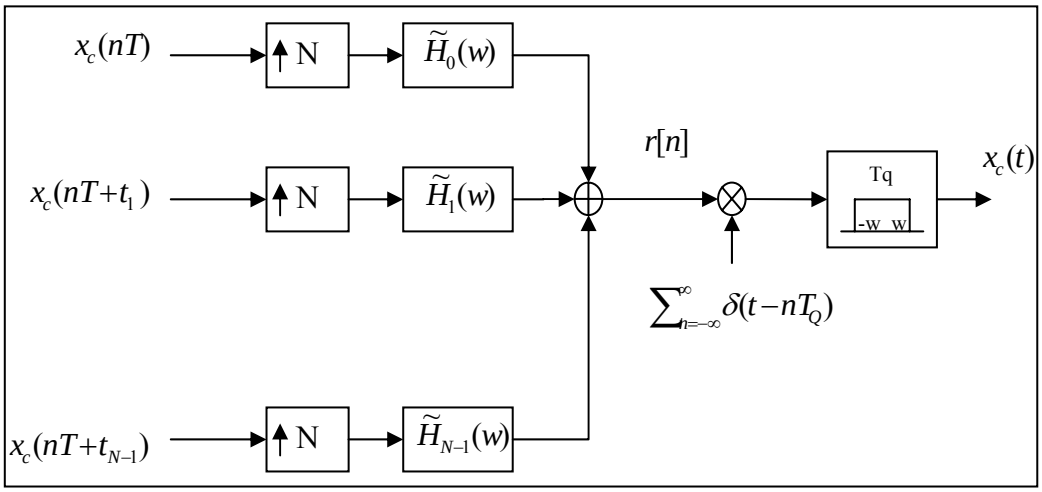

Figure 3.4: The discrete time equivalent of analog filter bank

When the final target of processing is the reconstruction of the analog signal $x_c(t)$ from its nonuniform samples $x_c(nT + t_p)$, the processing should be continued until the low pass filtering after the impulse modulation. Since in our case, it is the digital uniform samples that are required, the processing will be stopped when $r[n]$, the uniform samples, is obtained.

3.1.2. Nonuniform decimation approach

Efficient implementations are also possible with other approaches than the one represented by Oppenheim and Eldar. Of the most interesting ones are related to multirate techniques based on nonuniform decimation approaches. Vaidyanathan in a number of places [19], [20], [21], [22] refers to sampling expansions such as nonuniform sampling, each utilized by a multirate filter bank approach. The interested readers can find more, from many papers by Vaidyanathan on this approach, a tutorial [35] can also be useful. The advantages and disadvantages of multirate nonuniform decimation approaches are as summarized below.

Multirate techniques are efficient when compared to the classical algorithms based interpolations. Several applications are most conveniently implemented by filter bank approaches; therefore the ability to represent nonuniform sampling and reconstruction by utilizing multirate techniques is an absolute necessity. However a close analysis of multirate techniques for the nonuniform implementations reveals that, multirate techniques do not offer any performance gain over the classical closed form solutions, except for the computational efficiency. In general as can be seen from the related references, nonuniform decimation decimates a signal by N and uses only N-k channel signals for reconstruction, where those N-k samples carry the necessary Nyquist rate information of the signal: in other words the original signal is up sampled by at least N/N-k times the original Nyquist rate.

3.2 Results of the efficient filter bank implementation

The following figures show the obtained channel filters' frequency responses for a filter length of 64. The number of channels was eight, so that a reasonable number of filters can be shown. Two typical set of plots are given, that the change of the filter characteristics with respect to sample point distribution can easily be visualized. The figures represent the multilevel structure of the corresponding channel filters. The ripples are also recognized easily. The reason of the ripples is the rectangular window that is used to truncate the infinite length channel impulse responses.

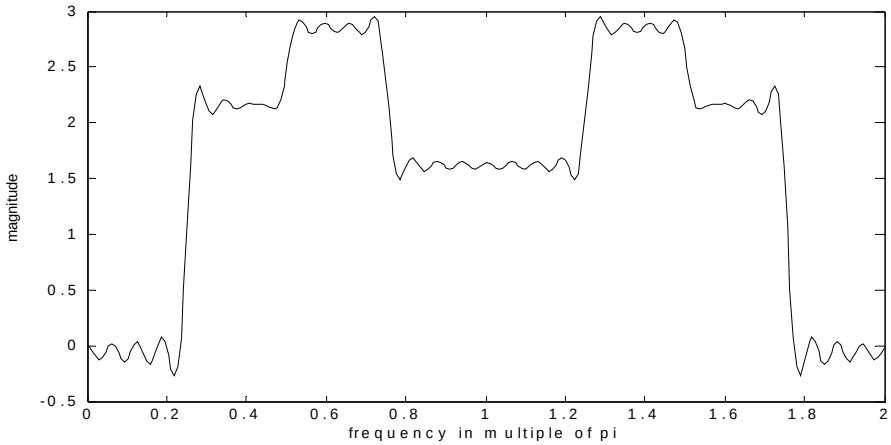

Figure 3.5.a1: Channel filter no 1

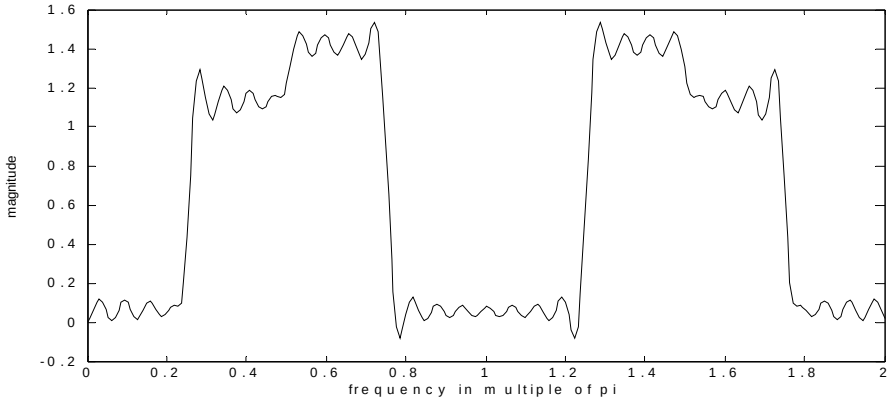

Figure 3.5.a2: Channel filter no 2

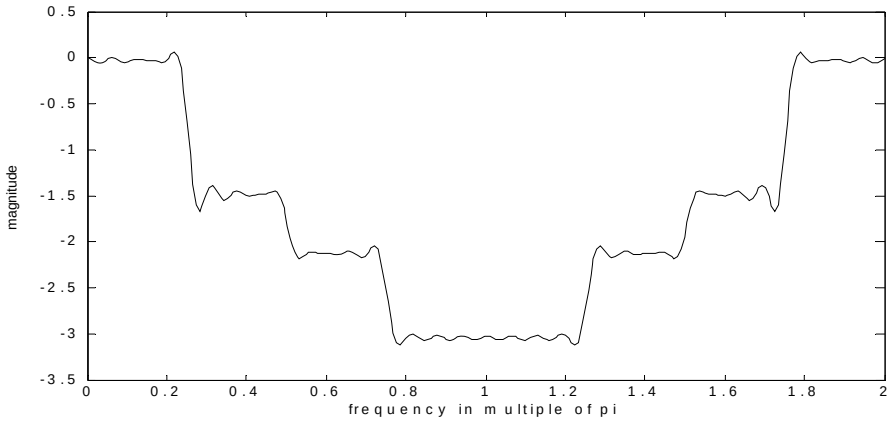

Figure 3.5.a3: Channel filter no 3

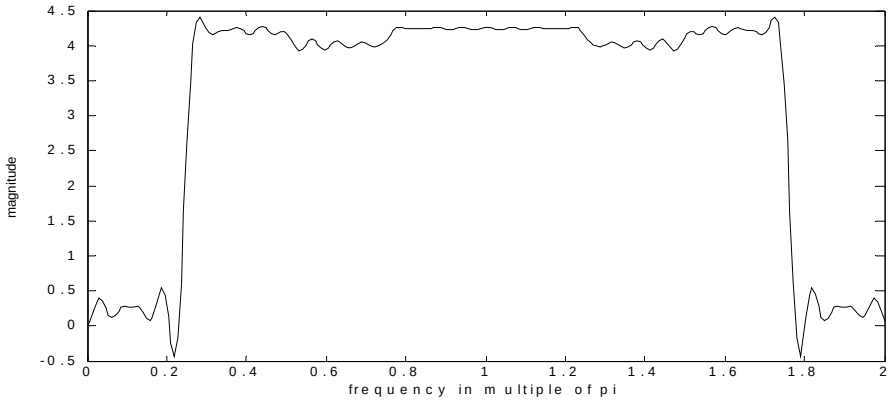

Figures 3.5.a4: Channel filter no 4

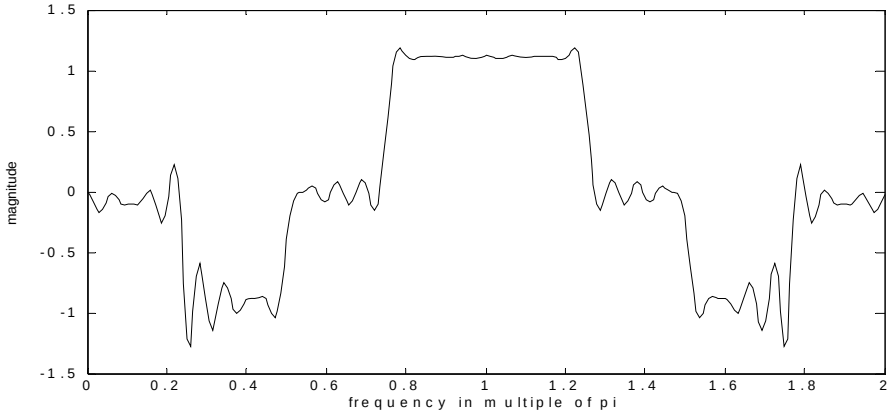

Figure 3.5.a6: Channel filter no 6

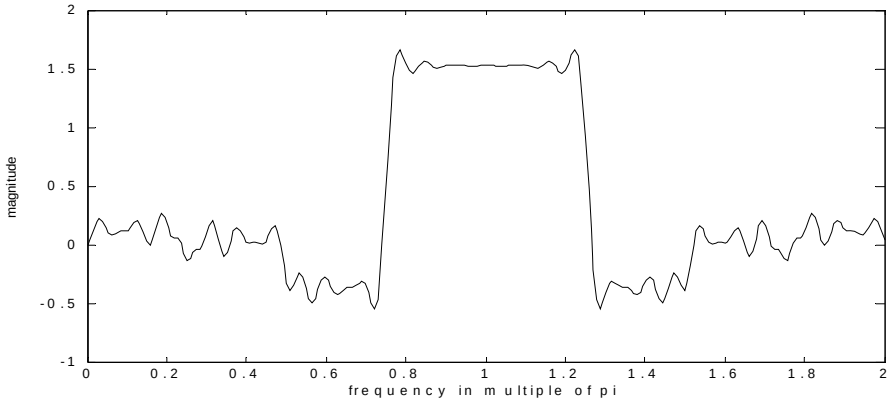

Figure 3.5.a6: Channel filter no 6

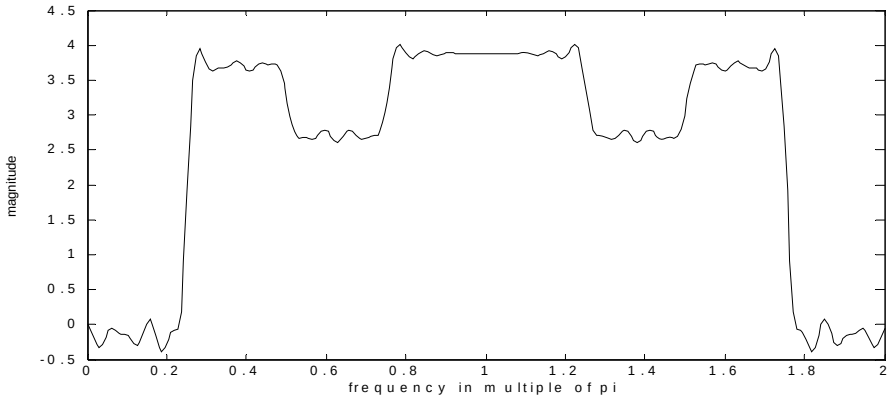

Figure 3.5.a7: Channel filter no 7

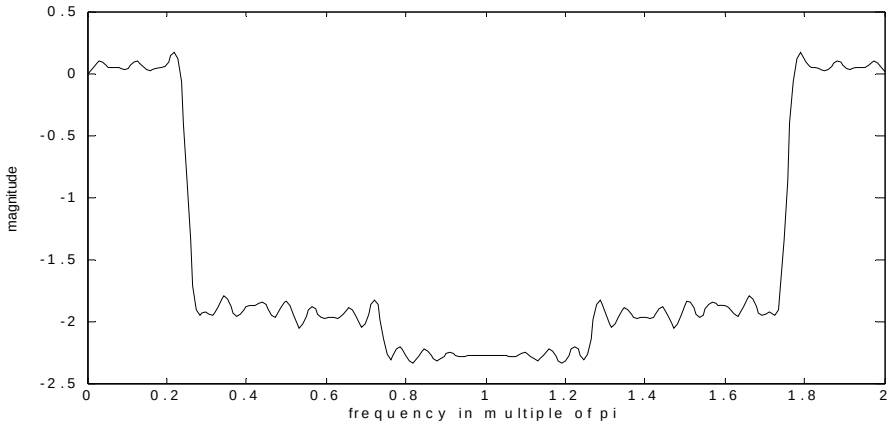

Figure 3.5.a8: Channel filter no 8

Next set of figures show the filters for a new sampling point distribution.

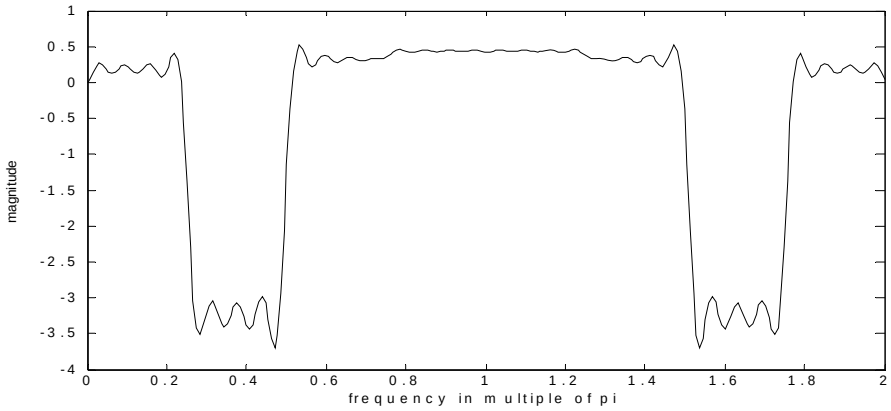

Figure 3.5.b1: Channel filter no 1

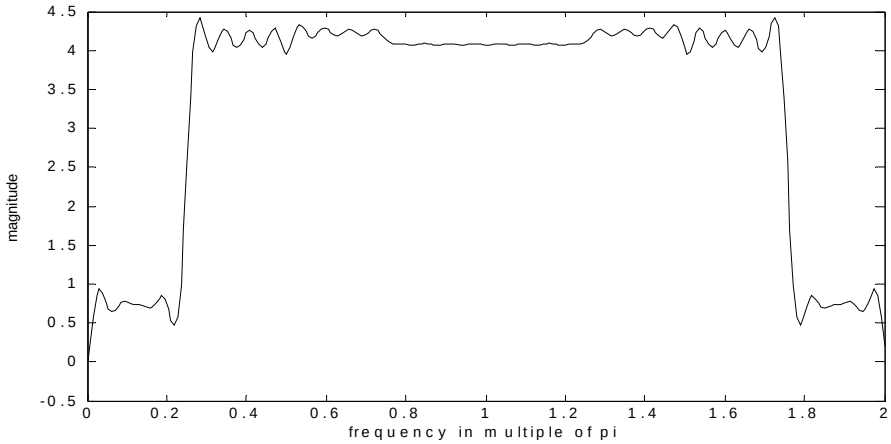

Figure 3.5.b2: Channel filter no 2

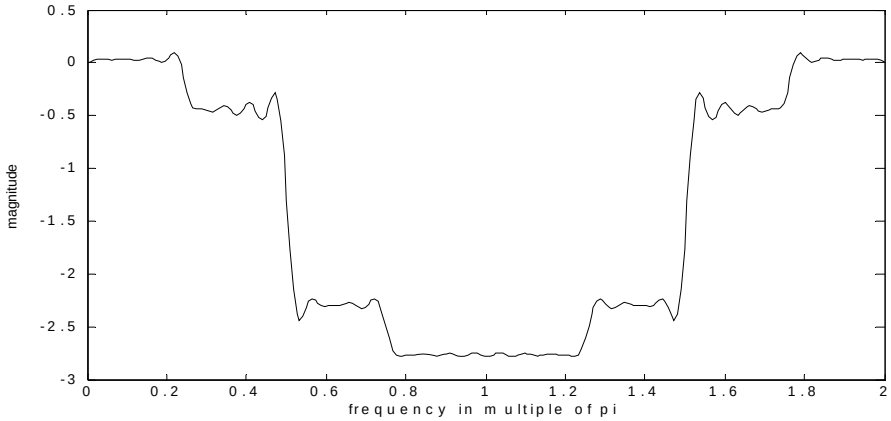

Figure 3.5.b3: Channel filter no 3

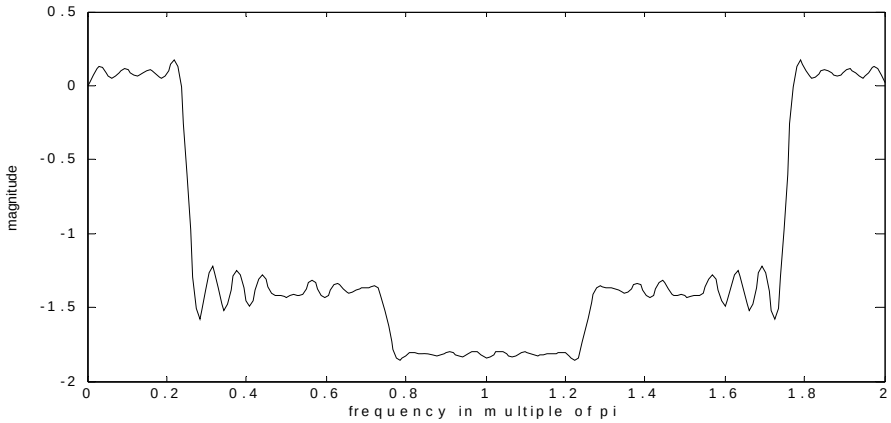

Figure 3.5.b4: Channel filter no 4

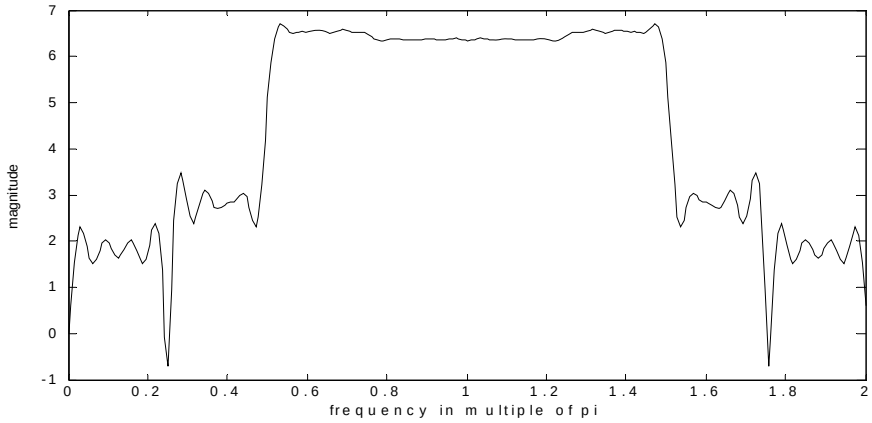

Figure 3.5.b5: Channel filter no 5

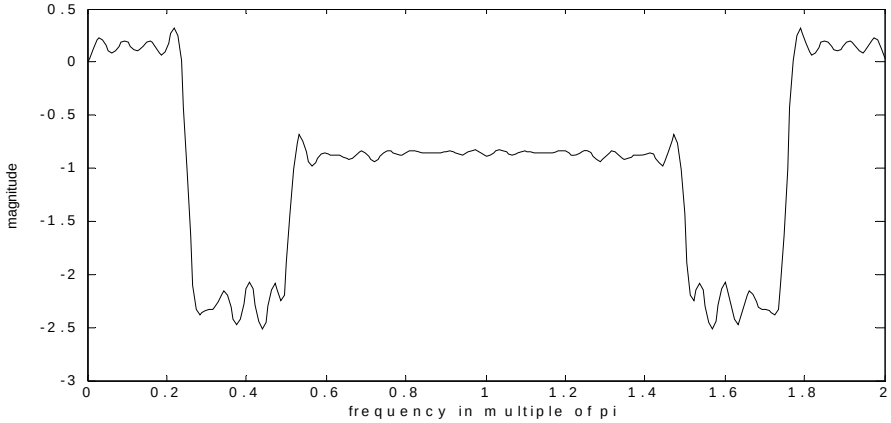

Figure 3.5.b6: Channel filter no 6

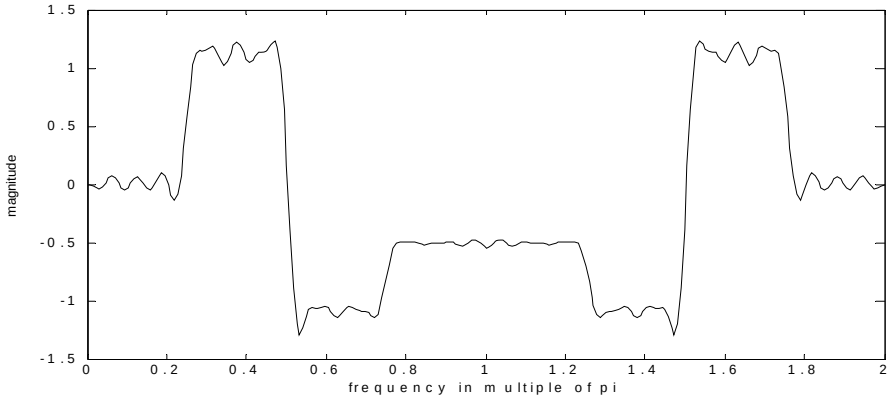

Figure 3.5.b7: Channel filter no 7

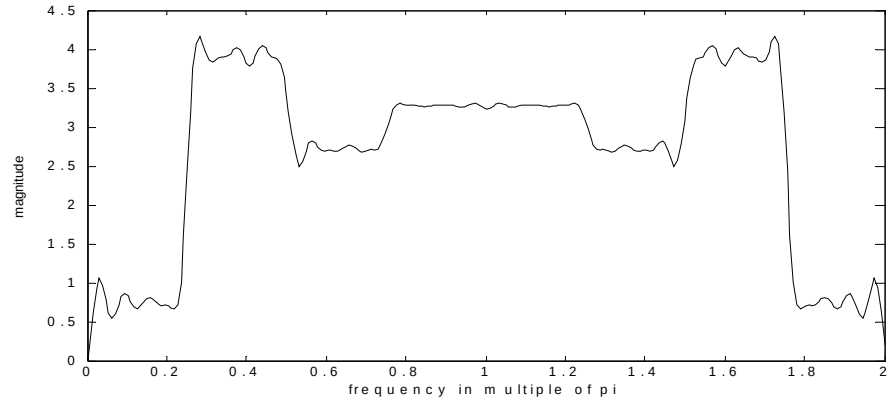

Figure 3.5.b8: Channel filter no 8

CHAPTER 4

RECONSTRUCTION ERROR VERSUS STABILITY

In chapter 2, classical closed form interpolation algorithms were described and their performances were tested with respect to changing signal and sampling conditions. In chapter 3, a computationally efficient implementation of recurrent nonuniform sampling algorithm was demonstrated. Its availability was an additional improvement on the performance of the algorithm. Now in this chapter the last criterion of interpolator analysis, the noise stability will be analyzed. First a definition of noise stability according to Yao and Thomas will be given. Then the reasons of a trade off algorithm are explained and the existing interpolators together with additional new ones are introduced. Finally their noise stability performance is simulated and the result is plotted.

4.1 Definition of reconstruction stability:

There is always unavoidable noise in the acquired sample values of a given analog signal. The source of the noise can be an additive noise on the signal as well as a measurement noise on the samples. In any case the sampling process will be erroneous. This will directly affect the reconstruction process. The noise on the measurement can drive the interpolator algorithms into unbounded, unstable outputs. This phenomenon, unlikely to happen in ordinary linear systems, can occur in systems like the interpolators. Therefore care should be given to stability analysis of interpolators. According to the references [1], [23], [24] the reconstruction stability, in the sense of Yao and Thomas, can be stated as follows.

An interpolator is said to be unstable in the BIBO sense if a small amount of noise present at the input generates a larger amount of noise at the output. Hence the SNR at the output is decreased, the noise is amplified and the interpolator harms the signal. The reason of such a behavior can be stated as the following. Every interpolator is designed to work for a given sampling rate, which defines the band limit of the input signals. If any input violates the band limit of the interpolator, then the well known aliasing error occurs. The classical approach to guarantee alias free operation is to simply anti alias filtering at the input of the sampling, prior to acquiring the samples of the signal. However, as the noise on the measurement may not occur at the input, but at the postsampling stages, such noisy components (especially resulting from the measurement error, quantisation error or electronic hardware noise) cannot be anti aliased by filtering only the input. Those noisy components will eventually introduce wide band error noise and this noise can accumulate. If we consider the frequency domain representation of signals and sampling, any signal component that exceeds the Nyquist frequency will overlap at the baseband. And hence the output noise power will be larger than the input noise power.

Another reason of reconstruction instability is exclusively related to nonuniform interpolation. When nonuniform sampling is considered, the sampling instants can tend to be as close as possible in analog precision. In general the theories put no restriction on such *bunching* of sampling points. However it is noted about such issues that when bunching happens, the corresponding *interpolation kernels* are likely to be unbounded at the intersample times. This phenomenon is not observed for uniform sampling. And such unbounded, very large actually, values may yield errors at the interpolator output. Yen in [17] presents a nice illustration to see such kernels and their unboundedness reason. For bandlimited signals such unbounded composing functions are unlikely to occur for an arbitrary sampling point distribution, however when there is wideband noise on the measured samples then the closer sampling points may eventually introduce unbounded results on the composing functions. The same is likely to occur if low resolution quantisation is applied.

4.2 The reasons and approach of trade off analysis

Ying and Munson [24] represent a tradeoff analysis that is based on the noise stability versus reconstruction accuracy of Yen's sinc kernel based arbitrary nonuniform sampling algorithm. The reason of the tradeoff approach taken in [24] can be explained as follows. Interpolation from nonuniform samples can take a variety of forms. One of those forms is the prominent sinc based interpolation kernel (See section 2.4.4). In general a sinc kernel based, practically time and bandlimited, interpolation can be put in a form such as the following.

$$\widetilde{x}_L(t) = \sum_{m=1}^{L}\sum_{n=1}^{L} \gamma_{mn} x(t_n) \frac{\sin(\sigma(t-t_m))}{\pi(t-t_m)} \tag{4.1}$$

where γ_{mn} is the (m,n)th element of a matrix, that is the inverse of another matrix Φ whose elements are defined according to (4.2).

$$\Phi(i,j) = \phi_{ij} = \phi(t_i, t_j) = \frac{\sin(\sigma(t_i - t_j))}{\pi(t_i - t_j)} \tag{4.2}$$

where $\sigma = 2\pi W$, with W the signal band width, and γ_{mn} are the elements of Φ^{-1}. Therefore the interpolation of a practically time and bandlimited signal from its nonuniform samples, in general, requires a matrix inversion.

According to noise stability criterion, an existing noise on the samples can result in an ill conditioned matrix whose inverse is difficult to compute, an unstable unbounded inverse that will yield an unstable interpolation. To solve this ill conditioning problem there exists proposed methods. The methods generally employ the idea of restricting the matrix Φ^{-1} so that the coefficients of the interpolation will not be ill conditioned.

The different methods of trade off analysis are distinguished from each other; by the way they impose restrictions on the Φ^{-1}, or the Φ , matrix.

In the next section, different proposed methods will be defined, their respective positions in the trade off will be explained and a new method described by Munson will be explained. Also Yen's RNS and FNS algorithms will be added to the stability test so that we may have a better comparison between each interpolator and we may see the RNS algorithm's noise stability performance.

4.3 Algorithms for noise stability versus reconstruction accuracy

4.3.1 Simplified sinc based interpolation

Jacobian interpolation takes equation (4.1) and replaces it by (4.3). In doing so the double summation loop is replaced with a single summation loop. Also the number of coefficients required to do the interpolation is decreased from L^2 into L. As can be seen, intersample and intercoefficient multiplications that exist in (4.1) have been eliminated.

$$\tilde{x}_L(t) = \sum_{i=1}^{L} c_i x(t_i) \frac{\sin(\sigma(t-t_i))}{\pi(t-t_i)} \tag{4.3}$$

with $c_i = t_i - t_{i+1}$ (4.4)

The algorithm creates a loss in the interpolation accuracy while the stability and computational efficiency, compared to double summation loop with matrix inversion, is assumed to increased.

4.3.2 Improved sinc based interpolation

Choi uses equation (4.3) suggested by Jacobian but with an improved coefficient calculation. The suggested interpolation coefficients are defined as

$$c_i = \frac{\phi_{ii}}{\sum_{j=1}^{L} \phi^2{}_{ji}} \tag{4.5}$$

where ϕ_i is from (4.2). This interpolator is claimed to be better than Jacobian and Yen interpolators for stability, however the accuracy is still far below the Yen interpolator.

4.3.3 Enhanced optimal sinc based interpolation

According to [24] the trade-off algorithm can be stated in brief as follows:

Assume an interpolation type as the one in (4.6)

$$\widetilde{x}_L(t) = \sum_{m=1}^{L}\sum_{n=1}^{L} b_{mn}\, x(t_n)\phi(t,t_m) \tag{4.6}$$

with $\phi(t,t_m) = 2W \sin c(2W(t-t_m))$

Where the coefficients b_{mn} are the elements of a symmetric matrix B to be designed. Indeed, B is derived from Φ as previously applied, however with a different point of view, which suggests a greater control over the interpolation coefficients b_{mn}, hence a control over the reconstruction stability and accuracy.

To set a beginning to the trade off, a measure of error vs. stability should be defined. The algebra associated with such a model can be quite complicated as demonstrated in [24], however the essence can be summarized as follows:

Choi and Munson [25] has shown a worst case error for (4.6) type interpolators as

$$\sup\left\|x-\tilde{x}_L\right\| = \sqrt{1-\lambda_{\min}} \tag{4.7}$$

with $\lambda_{\min}$ being the minimum egienvalue of matrix $2\Phi B-(\Phi B)^2$. And they also indicated that the above minimization is equivalent to finding the matrix B, which minimizes $\left\|\Phi B-I\right\|_2$ with $\left\|\cdot\right\|_2$ being the spectral norm. Since minimization of spectral norm is difficult, another norm, the Frobenius norm is used to minimize the quantity. Hence the solution will be an approximate one. The algorithm then follows: The norm is expanded and

$$\left\|\Phi B-I\right\|_F^2 = \sum_i (\sum_k \phi_{ik} b_{ki} - 1)^2 + \sum_{i\neq j}\sum_j (\sum_k \phi_{ik} b_{kj})^2 \tag{4.8}$$

the derivative with respect to b_{mn} is set to zero, resulting in

$$\sum_k \sum_i \phi_{ik}\phi_{im} b_{kn} + \sum_k \sum_i \phi_{ik}\phi_{in} b_{km} = \phi_{mn} + \phi_{nm} \tag{4.9}$$

Equation (4.9) is the equation that describes the solution of B matrix, in terms of its coefficients. Therefore to find the corresponding interpolation coefficients, (4.9) should be solved. Note that (4.9) indeed represents the Yen and the Choi interpolators. Yen interpolator uses all of the b_{mn} coefficients hence requires the full solution of (4.9). Whereas the Choi interpolator uses only the diagonal entries of matrix B by setting $bij = 0$ for $i \neq j$, hence requires the solution for the remaining b_{mm} of (4.9). What is suggested by the trade-off is the following.

a- For better conditioning, set, more off diagonal entries of B to zero and solve for the remaining b_{mn} from equation (4.9).

b- For better accuracy, up to Yen interpolator , set, less diagonal entries to zero.

Indeed for optimal accuracy solve all b_{mn} as $B = \Phi^{-1}$ which is the Yen 4 solution.

The tradeoff algorithm requires the following operations.

1- Define the diagonals of symmetric weighting matrix B, whose elements are interpolation coefficients according to (4.6), by labeling them as k^{th} diagonal.

2- Decide on a k value between 1 and L on the basis of a trade-off comparison.

3- Optionally search for an optimal k**,** in the sense of an optimal balance between accuracy and noise stability. One such optimality condition can be found in [24] as follows:

Provided that SNR is known and the sampling grid is fixed, a worst-case error can be given as:

$$\varepsilon(k) = \sqrt{1 - \lambda_{\min}(k) + tr(k)10^{-\frac{SNR}{10}}} \qquad (4.10)$$

And the optimal k is the one that minimizes (4.10).

The minimization can be done by a number of known techniques. Alternatively Appendix D shows a structured way of finding the optimal k according to equation (4.10)

5-After deciding on the value of k, the next step is to solve the equation (4.9) in an appropriate manner. This can be accomplished in two different ways; the first belongs to the authors of [24]. The second solution is obtained by modifying the algorithm suitable for fast computational solutions, the detailed derivation of finding the weighting coefficients b_{mn} can be found in appendix D.

4.3.4 Optimal sinc based interpolator

Optimal sinc based interpolation was discussed in chapter 2, [Yen 4]. The algorithm is based on the minimization of the reconstruction error. The details can be seen from section (2.1.4). The resulting interpolator will try to yield minimum reconstruction error for noise free signals.

4.3.5 Modified recurrent nonuniform interpolator

Recurrent nonuniform sampling was described in section (2.1.3) where the algorithm assumed a period of N and infinite number of periods. However from a practical point of view we can restrict the number of periods to be one, hence only one period of N samples is interpolated. The performance of this algorithm is not affected from such a modification and yielded very good results.

4.4 Stability simulation results

In the test, SNR is incremented in steps of 6 dB and interpolation is repeated for 20 times to smooth the MSE. The signal used was the same signal used in A1, with the same characteristics. The trade off algorithm is included with a *fixed* k parameter of 25, where the signal length is 50 samples. The fact that the k parameter is fixed actually eliminates us to view the dynamic behavior of the minmax interpolator, however when stability in the sense of Yao and Thomas is considered, noise amplification is always present for any value of k. Because the upper limit of k, which is equivalent to Yen interpolator has inherent noise amplification. From the figure, two things are apparent: RNS of Yen displayed a superior noise behavior compared to the other algorithms. It is also clear that Yen 's sinc based interpolator shows some amount of noise amplification, which is seen from the flattening portions of the plot. As SNR gets higher, only Yen 1 and 3 can survive to generate a linear MSE with SNR. The other algorithms show amplified noise at their outputs. However it is observed that the trade off approach did not present what it claimed. Noise is always amplified.

It was not more stable than the Yen 4 especially at high SNR. And it was only as stable as Yen 4 for low SNR.

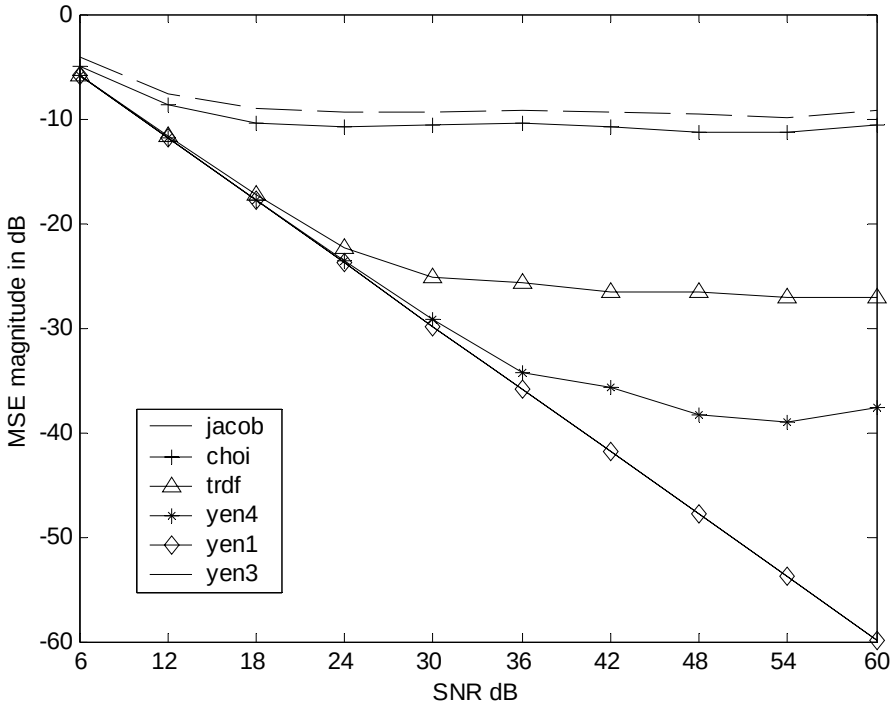

Figure (4.1): MSE versus SNR for interpolation of the time and bandlimited signal according to noise stability criteria.

Looking at the figure 4.1 one important characteristic of all interpolators is also observed. It is understood from the figure that, each sinc based interpolator has an upper limit of interpolation accuracy whether there exist any noise or not. This is observed from the flattening portion of mse curves. Those flattening portions indicate that, no matter how large the SNR, (how small the noise power) the interpolation error will not be less than a given minimum value. This minimum value of interpolation error can be stated as the absolute performance of each interpolator. For example the absolute performance of Choi algorithm is around –10 dB, whereas ANS (Yen 4) has around –40dB. Also seen from the plot is that RNS and FNS do not exhibit a flattening portion. Since their absolute performance is less than –120 dB, which is not reached by the test, so that could not be observed. (See figure 2.7 for their absolute performance curves of RNS and FNS)

CHAPTER 5

CONCLUSIONS

5.1. Conclusions on reconstruction accuracy

The simulation results indicate the followings. Yen algorithm 3, recursive nonuniform sampling, represented a superior interpolator characteristics. It is apparent from the relevant LSE plots, that RNS represents an almost linear LSE with increasing SNR. So it is simply verified once more that RNS is insensitive to noise on the samples. In addition RNS shows as little as –120 dB LSE error and it can also display even better results, as SNR gets larger and larger. What else is apparent from the figures that ANS, Yen 4, shows a considerably less accurate interpolation, when compared to RNS. In fact ANS shows a minimum error of –40 dB after a value of SNR is reached. Then the LSE of ANS stops responding to SNR value of the input and shows a highly nonlinear flat LSE curve. This flat portion of the LSE curve can be called as the absolute performance threshold, that upon which SNR has no effect on the output LSE. Very strong noise amplification is present on those flat portions of the LSE curves. As a result it is verified that Yen 3 can realize a perfect reconstruction from arbitrary nonuniform samples, whereas Yen 4 is not close to a perfect reconstruction algorithms, even for a time and band limited input signal.

Also as the result of sample point distribution tests indicate, RNS algorithm has proved insignificant dependence on the sample point distributions when compared to ANS. As seen from the respective figures, ANS exhibits considerable dependence on the sample point distribution for a given fixed signal. This clearly indicates a numerical problem associated with ANS, however this problem did not cause severe conditioning.

Also observed is the fact that as the sample point deviation variance gets larger and larger, the error tends to reach a limit value. This is due to the reason that every sample is registered to the system with its corresponding sampling instant. As long as explicit sampling instants are known, crossovers will not generate that much of a problem. The maximum amount of error occurs in two sample distribution conditions. In the first case points are distributed such that very close sampling instants occur, whereas in the second case the sampling grid reaches its maximum average deviations from the uniform instants.

The missing sample problem is also considered and as the simulations shows, RNS algorithm can withstand at most two missing samples with moderate errors. The error for two missing sample was around –50dB, whereas the error for three missing samples was much worse, around –20dB. Hence, it can be stated that RNS can hold at most a two sample miss at a signal length of 50 samples.

5.2 Conclusions on computational efficiency

In simplest considerations, the complexity of the Yen's interpolators can be stated as follows. A complexity of $O(N^2)$ is always present due to the interpolation summation equation that all interpolators do have.

FNS uses a very complicated composing function, which requires at least 4N sinusoidal multiplications to be computed for a specific time and index. Therefore, the complexity of FNS is expected to be $O(N^3)$ for all outputs to be computed. SINS uses gamma function for interpolation. The composing function requires no loops. Therefore total complexity for interpolation of N samples can be put as $Gamma * O(N^2)$, where Gamma stands for gamma function complexity. RNS algorithm uses a moderate complexity composing function, which requires N multiplications to be calculated.

Therefore the complexity of it is expected to be $O(N^3)$. ANS algorithm employs a two step interpolation computation. The first step is the computation of B matrix and the next step is the computation of output samples. It requires the creation and inversion of a matrix of size N^2. In addition a complexity of $O(N^3)$ for interpolation exists. As a result the expected order of computational complexities can be stated as follows. SINS, RNS, FNS, ANS

Filter bank approach converted the RNS algorithm into a much faster linear filtering algorithm. The complexity is decreased by orders of magnitude, especially at high N values. The drawback of filter bank approach however is a delay associated with the output samples. Therefore RNS algorithm is very suitable for fast, efficient computations as well as accurate interpolations.

5.3 Conclusions for noise stability

The test results on noise stability indicate that although ANS of Yen, displayed noise amplification at high SNR values, the proposed tradeoff solution, introduced more noise amplification than the Yen 4. In addition, its interpolation accuracy was below the ANS. Therefore, based on our experiments and observations, it can be stated that arbitrary nonuniform sampling strategy displays no interpolation instability, in the sense of Thomas and Yao, compared to the tradeoff approach. However what we discovered, more importantly than the above, is the existence of RNS and FNS algorithms as solid, superior, noise immune interpolation algorithms, exhibiting linear MSE with increasing SNR. This fact forms our conclusion on noise stability as follows. RNS algorithm performs the best noise stability characteristics. Its output MSE decays linearly with increasing SNR, which means that no noise amplification is present. It is observed that RNS is more robust than both ANS and trade off algorithms. The trade off approach offered no observable advantages over ANS or RNS.

REFERENCES

[1] Abdul J. Jerri, "The Shannon Sampling Theorem-Its Various Extensions and Applications: A Tutorial Review", proceedings of IEEE vol.65, no.11, November 1977

[2] D.L.Jagerman, L.J. Fogel, "Some general Aspects of the Sampling Theorem" IRE transactions on information theory, December 1956

[3] Claude E. Shannon," Communication in the presence of noise ", classic paper (excerpt from " proceedings of IEEE vol. 86, no.2, February 1998 ")

[4] H. Nyquist, "Certain topics in telegraph transmission theory" AIEE Trans.,vol. 47, pp. 617-644, 1928

[5] E.T. Whittaker, " On the functions which are represented by the expansion of interpolating theory" , Proc. Roy. Soc. Edinburgh, vol. 35, pp. 181-194, 1915.

[6] J.M. Whittaker, " The Fourier theory of the cardinal functions ", Proc. Math. Soc. Edinburgh, vol. 1, pp.169-176, 1929.

[7] J.M. Whittaker, " Interpolatory Function Theory", Cambridge England: Cambridge University Press (Cambridge tracts in Mathematics and Mathematical Physics) , 1935, no.33

[8] W.L. Ferrar ," On the consistency of cardinal function interpolation", Proc. Roy. Soc. Edinburgh, vol. 47, pp. 230-242, 1927.

[9] Frederic J. Beutler ,"Alias-Free Randomly Timed Sampling of stochastic processes", IEEE Transactions on information theory, vol. IT-16 no. 2, march 1970

[10] F.J. Beutler, " error free recovery of signals from irregularly spaced samples", SIAM Rev., vol. 8, pp. 328-335, 1966

[11] S.P. Lloyd, "A sampling theorem for stationary (wide sense) stochastic processes", Trans. Am. Math. Soc., vol. 92, pp. 347-363, 1966

[12] Weiss, "Sampling theorems associated with Strum-Liouville systems", Bull. Math. Soc., vol. 63, p.242 (abstract 459) 1957

[13] H.P. Kramer, "A generalized sampling theorem", J. Math. Phys., vol. 38, pp. 68-72, 1959

[14] L.L. Campell "A comparison of the sampling theorems of Kramer and Whittaker" J. SIAM, vol.12, pp.117-130, 1964.

[15] D.Slepian and H.O. Pollack ,"Prolate spheroidal wave functions, Fourier analysis and uncertainity-I", Bell. syst. tech. Journ., vol. 40, pp. 43-64, 1961

[16] A.J. Jerri, "On the application of some interpolating functions in physics", J. Res Nat. Bur. Stand. –B. Math. Scienc. , vol 73B, no.3, pp.241-245 sept. 1969

[17] J.L.Yen "On Nonuniform Sampling of Bandwidth-Limited Signals", IRE transactions on circuit theory, vol CT-3, pp.251-257 Dec 1956

[18] Oppenheim, Eldar ," Filter bank Reconstruction of Bandlimited Signals from Nonuniform and Generalized Samples", IEEE trans. on signal processing, vol.48, no 10, October 2000

[19] Vrcelj, Vaidyanathan, "efficient implementation of All-Digital Interpolation", IEEE trans. on image processing, vol 10, no. 11, November 2001

[20] P.P.Vaidyanathan, "Efficient Reconstruction of Band-Limited Sequences from Nonuniformly Decimated Versions by Use of Polyphase Filter banks", IEEE trans. on acoustics. Speech. and Signal processing, vol. 28, n. 11, November 1990

[21] P.P. Vaidyanathan, " Periodically Nonuniform Sampling", IEEE Trans. on Circuits and Systems-II analog and Digital Signal Processing, vol. 45, No. 3, March 1998

[22] P.P. Vaidyanathan, "Generalizations of the Sampling Theorem: Seven decades after Nyquist". IEEE Trans. on Circuits and Systems-I Fundamental Theory and applications, vol. 48, No. 9, September 2001

[23] Yao and Thomas, "On Some Stability and Interpolatory properties of Nonuniform sampling expansions", IEEE Trans. on Circuit Theory, vol CT-14, no 4, December 1967

[24] L.Ying and D.C. Munson, Jr., “Approximation of minmax interpolator”, Proceedings of IEEE International Conference on Acoustics, Speech and Signal Processing 2000, vol.1, pp. 328-331, June 2000

[25] Choi Munson Jr.,"Analysis and design of minmax optimal interpolators", IEEE Trans. Signal Processing ,vol.46, pp 1571-1579, 1998

[26] J.E. Whitehouse and S.J.Sangwine, " The sampling theorem-a tutorial" IEE 1994

[27] Hans dieter Lüke, "The origins of Sampling Theorem", IEEE Comm. Magazine, April 1999

[28] Davis. M. Artice, "Almost periodic extensions of band-limited functions and its application to Nonuniform sampling", IEEE Trans. on Circuits and Systems. Vol. Cas-33, No. 10, October 1986

[29] E.V.D. Ouderra and J. Renneboog, "Some Formulas and applications of Nonuniform Sampling of Bandwidth limited Signals", IEEE Trans. on Instrm. and Measurement. vol. 37, No. 3, September 1988

[30] A. Papoulis, "Generalized Sampling Expansion" IEEE Trans. Circuits and Systems. Vol. CAS-24, pp.652-654, Nov 1977

[31] F.Marvasti, M.Analoui, and M. Gamshadzahi, "Recovery of signals from nonuniform samples using iterative methods" IEEE Trans. Signal Proc., vol. 39, pp 872-877, Apr. 1991.

[32] R.G. Wiley, "Recovery of Bandlimited Signals from Unequally Spaced Samples", IEE Trans. on Commun., vol. COMM-26, pp.135-137, Jan. 1978

[33] Donald Fraser, " Interpolation by the FFT –Revisited- An Experimental Investigation", IEEE Trans. on Acoustics Speech and Signal Proc. Vol. 37, No.5. May 1989.

[34] T.J. Cavichi, "DFT time-domain interpolation", IEEE proc.-F,Vol.139, No.3, June 1992

[35] P.P. Vaidyanathan and V.C. Liu, "Classical sampling theorem in the context of multirate and polyphase digital filer bank structures", IEEE Trans. Acoust., Speech., Signal Procssing. vol 36, pp.1480-1495, Sept.1988

[36] A.V. Oppenheim, R.W Schaffer and J.R. Buck, "Discrete Time signal processing , second edition" Englewood Cliffs, NJ: Prentice Hall, 1999

[37] E.C. Tischmarsh, "The Theory of Functions, second edition" Oxford U.K.: Oxford Univ. Press, 1939.

Appendix A

Lagrangian interpolatory theory and proof of GST

A.1 Lagrangian interpolation

From linear algebra it is known that when the values of a function are known at a set of points, (let them be $f(t_0), f(t_1),..., f(t_n)$) then the respective continuous function $f(t)$ can be exactly constructed as a finite degree, degree n, polynomial. The function has the property that it is the minimum degree polynomial that passes through all the supplied data points. A larger degree polynomial can also satisfy the conditions but will loose uniqueness.

A polynomial of nth degree is exactly specified by $n+1$ points and has n zeros. The lagrangian interpolation is the following form

$$P_n(t) = f_0 L_0^n(t) + f_1 L_1^n(t) + ... + f_n L_n^n(t) \qquad \text{(A.1)}$$

where $f_n = f(t_n)$ and the Lagrangian Coefficient is defined by $L_i^n(t)$

$$L_i^n(t) = \frac{(t-t_0)(t-t_1)...(t-t_{i-1})(t-t_{i+1})...(t-t_n)}{(t_i-t_0)(t_i-t_1)...(t_i-t_{i-1})(t_i-t_{i+1})...(t_i-t_n)} \qquad \text{(A.2)}$$

Note that this Lagrangian Coefficient has the important property that it is "selective", meaning

$$L_i^n(t_j) = 0, \quad i \neq j \qquad \text{(A.3)}$$
$$= 1, \quad i = j$$

In order to further manipulate the lagrangian interpolation, the lagrangian coefficient can be written as follows.

Let $g_n(t)$ be defined as

$$g_n(t) = (t - t_0)(t - t_1)...(t - t_n) \tag{A.4}$$

then the lagrangian coefficients can be written in the form of

$$L_i^n(t) = \frac{g_n(t)}{(t - t_i)g_n'(t_i)} \tag{A.5}$$

And the Lagrangian Interpolation Polynomial becomes

$$P_n(t) = g_n(t)\sum_{i=0}^{n} \frac{f_i}{(t - t_i)g_n'(t_i)} \tag{A.6}$$

At this point complex z is introduced for a simple mathematical generalization that is better expressed in complex domain. However, the real variable will be inserted wherever possible.

$$\frac{P_n(z)}{g_n(z)} = \frac{f_0}{(z - z_0)g_n'(z_0)} + \frac{f_1}{(z - z_1)g_n'(z_1)} + ... + \frac{f_n}{(z - z_n)g_n'(z_n)} \tag{A.7}$$

(1.7) shows the properties that will lead into a generalization and the number of points will become infinite.

Both functions in the left hand side of (1.7) are entire, and denominator vanishes at the sampling instants. When the required manipulations are applied (not shown in ref [2]) the Lagrangian interpolation can be invoked for an infinite number of sample points. This point initiates the more modern approach of cardinal series. A suitable choice of an entire function $g_n(z)$, which vanishes at a countable number of infinite equidistant points is

$$g(z) = \sin(\frac{\pi}{h} z) \tag{A.8}$$

Where the subscript n is dropped. Replacing complex z with real t, we find the required function

$$g(t) = \sin(\frac{\pi}{h}t) \tag{A.9}$$

This function has zeros uniformly distributed in t axis, at $t = kh$ $k = ...,-2,-1,0,1,2,...$.Hence equation (A.6) can be rewritten in terms of $g(t)$ as follows

$$\sin(\frac{\pi}{h}t)\sum_{i=-\infty}^{\infty}(-1)^i \frac{f_i}{(t-t_i)} \tag{A.10}$$

At this point finally (A.10) can be rewritten to represent the familiar interpolation cardinal series with sinusoidal kernel. An entire function $f(t)$ is given by the following series

$$f(t) = \sum_{i=-\infty}^{\infty} \frac{\sin(\pi/h)(t-ih)}{(\pi/h)(t-ih)} \tag{A.11}$$

h should satisfy the well known condition $h \le 1/2W$ where W is the bandwidth of the bandlimited function $f(t)$

A2. Proof of generalized sampling theorem

The simplest proof of the GST theorem can be stated as follows:

1- writing down the orthogonal expansion of the function g (x) in equation (1.7).

$$g(x) = \sum_{n=1}^{\infty} c_n \overline{K(x,t_n)} \tag{A.12}$$

2- using the linear space orthogonality relations, c_n can be written as follows:

$$c_n = \frac{\int_I g(x)K(x,t_n)dx}{\int_I |K(x,t_n)|^2 dx} = \frac{f(t_n)}{\int_I |K(x,t_n)|^2 dx} \tag{A.13}$$

In the above, the upper integral had been evaluated version of equation (1.7) at t=t_n and yielded the result of $f(t_n)$. It could also be interpreted as the inner product equation for the space $L_2(I)$.

3- multiplying each side of equation. (A.12) by $K(x,t)$ and integrating term by term.

$$\int_I K(x,t)g(x)dx = \int_I K(x,t)\sum_{n=1}^{\infty} c_n \overline{K(x,t_n)}dx \qquad \text{(A.14)}$$

Interchange the order of summation integration to get (E.15)

$$f(t) = \sum_{n=1}^{\infty} c_n \int_I K(x,t)\overline{K(x,t_n)}dx \qquad \text{(A.15)}$$

substituting the value of c_n found in equation. (A.13) into equation. (E.15) we get equation.(A.16)

$$f(t) = \sum_{n=1}^{\infty} \frac{f(t_n)}{\int_I |K(x,t_n)|^2 dx} \int_I K(x,t)\overline{K(x,t_n)}dx$$

(A.16)

grouping the integrals together, we see the form of equation. (1.9) in the right side

$$f(t) = \sum_{n=1}^{\infty} f(t_n) \frac{\int_I K(x,t)\overline{K(x,t_n)}dx}{\int_I |K(x,t_n)|^2 dx} \qquad \text{(A.17)}$$

hence, using equation. (1.9) we get the final and desired form.

$$f(t) = \sum_{n=1}^{\infty} f(t_n)S(t,t_n) \qquad \text{(1.8)}$$

Appendix B

Derivation of recurrent nonuniform sampling

Remembering section 1.1.1 Lagrangian interpolation was capable of yielding an explicit reconstruction formula for a general sample instant point distribution with the following result:

$$P_n(t) = g_n(t)\sum_{i=0}^{n}\frac{f_i}{(t-t_i)g_n'(t_i)} \qquad \text{(B.1)}$$

Where equation (1.4) is reproduced with a general number of samples as (n+1). In that section it is also shown what happens when n is forced to infinity. The interpolation formula can be put in a more structured way by allowing with sinc type bandlimited interpolation kernels. Another equivalent form of explicit reconstruction strategy that can be employed for any type of sampling point distributions that obey class 1,2 and 3, can also be put as the following, from reference [18],[36]

To reconstruct a continuous signal $x_c(t)$ from its samples, taken at sampling instants $\{t_n\}$, with the fact that average sampling period, $\lim_{n\to\infty}(t_n/n)$, is less than the Nyquist period, we have the following theorem:

Theorem B.1: " let $x_c(t)$ be a finite energy bandlimited signal such that $X_c(\Omega) = 0$ for $|\Omega| > W - \varepsilon$ for some $0 < \varepsilon \le W$. $x_c(t)$ is uniquely defined by its samples $x_c(t_n)$ if

$$\left|t_n - n\frac{\pi}{W}\right| < L < \infty$$

$$|t_n - t_m| > \delta > 0 \qquad n \neq m$$

The reconstruction is given by:

$$x_c(t) = \sum_{n=-\infty}^{\infty} x_c(t_n)\frac{G(t)}{G'(t)(t-t_n)} \qquad \text{(B.2)}$$

Where

$$G(t) = (t - t_0) \prod_{\substack{n=-\infty \\ n \neq 0}}^{\infty} (1 - \frac{t}{t_n}) \tag{B.3}$$

$G'(t)$ is the derivative of $G(t)$ evaluated at $t = t_n$ and if $t_n = 0$ for any n, then $t_0 = 0$.

Practical value of the above theorem will be evident, in the analysis of artificial nonuniformity definition that fall into class 3. Especially for sampling instants that result from forced definitions based on a set of numerical instants, we can find closed form explicit interpolation functions. Yen's algorithm 3, the recurrent nonuniform sampling and reconstruction can be derived from the above theorem, according to reference [13] as outlined below:

The complete sampling instants can be put as $\tau_{pn} = t_p + nT$ and inserting τ_{pn} into (B.3) we have

$$G(t) = t \prod_{\substack{n=-\infty \\ n \neq 0}}^{\infty} (1 - \frac{t}{nT}) \prod_{n=-\infty}^{\infty} (1 - \frac{t}{nT + t_1}) \ldots \prod_{n=-\infty}^{\infty} (1 - \frac{t}{nT + t_{N-1}}) \tag{B.4}$$

Every product term in (B.4) converges to a constant times $\sin(\pi(t - t_p)/T)$ which can be shown as follows using a very useful property [37] as the following

$$\sin(\pi t / T) = kt \prod_{\substack{n=-\infty \\ n \neq 0}}^{\infty} (1 - \frac{t}{nT}) \tag{B.5}$$

k being a constant. Thus it follows that

$$\sin(\pi(t - t_p)/T) = k(t - t_p) \prod_{\substack{n=-\infty \\ n \neq 0}}^{\infty} (1 - \frac{t - t_p}{nT})$$

$$= -k \prod_{n=-\infty}^{\infty} (nT - t - t_p) \prod_{\substack{n=-\infty \\ n \neq 0}}^{\infty} \frac{1}{nT}$$

$$= -kt_p \prod_{n=-\infty}^{\infty} (1 - \frac{t}{nT + t_p}) \prod_{\substack{n=-\infty \\ n\neq 0}}^{\infty} \frac{nT + t_p}{nT}$$

$$= -kt_p \prod_{n=-\infty}^{\infty} (1 - \frac{t}{nT + t_p}) \prod_{\substack{n=-\infty \\ n\neq 0}}^{\infty} (1 + \frac{t_p}{nT})$$

$$= -\sin(\pi t_p / T) \prod_{n=-\infty}^{\infty} (1 - \frac{t}{nT + t_p})$$

$$= \tilde{k} \prod_{n=-\infty}^{\infty} (1 - \frac{t}{nT + t_p})$$

hence (B.4) can be written as

$$G(t) = c \prod_{p=0}^{N-1} \sin(\pi (t - t_p) / T) \qquad \text{(B.6)}$$

c being and arbitrary constant. The derivative of (B.6) can be found as follows:

$$G(t_p + nT)' = c \frac{\pi}{T} \cos(\pi n) \prod_{\substack{q=0 \\ q\neq p}}^{N-1} \sin(\pi (t_p + nT - t_q) / T)$$

$$= c \frac{\pi}{T} (-1)^{nN} \prod_{\substack{q=0 \\ q\neq p}}^{N-1} \sin(\pi (t_p - t_q) / T) \qquad \text{(B.7)}$$

Substituting equations (B.7), (B.6) and $\tau_{pn} = t_p + nT$ into equation (B.2) will result in explicit reconstruction formula defined by Recurrent Nonuniform Sampling as in section (2.1.3) also the same as in (3.4) with a slight modification

$$f(t) = \sum_{m=-\infty}^{\infty} \sum_{p=1}^{N} f(\tau_{pm}) \frac{\prod_{q=1}^{N} \sin(\frac{2\pi W}{N}(t - t_q))}{\prod_{\substack{q=1 \\ q\neq p}}^{N} \sin(\frac{2\pi W}{N}(t_p - t_q))} \frac{(-1)^{mN}}{\frac{2\pi W}{N}(t - t_p - \frac{mN}{2W})} \qquad \text{(B.8)}$$

Appendix C

Derivation of analog filter bank for Yen algorithm 3

The development of the continuous time filter bank is as follows:

1- Replace the order of summations in the equation (3.3) to get (C.1)

$$x_c(t) = \sum_{p=0}^{N-1} \sum_{n=-\infty}^{\infty} x_c(nT + t_p) \frac{a_p (-1)^{nN} \prod_{q=0}^{N-1} \sin(\pi(t - t_q)/T)}{\pi(t - nT - t_p)/T} \qquad \text{(C.1)}$$

2- Denote the inner sum as $f_p(t)$:

$$f_p(t) = \sum_{k=-\infty}^{\infty} x_c(kT + t_p) \frac{a_p (-1)^{kN} \prod_{q=0}^{N-1} \sin(\frac{\pi}{T}(t - t_q))}{\frac{\pi}{T}(t - kT - t_p)} \qquad \text{(C.2)}$$

3- Using the relation $\sin(t - k\pi) = (-1)^k \sin(t)$ the above equation can be rewritten as a convolution operation**.** Specifically we have

$$f_p(t) = s_p(t) * h_p(t) \qquad \text{(C.3)}$$

where $h_p(t)$, p$^{\text{th}}$ analog channel filter impulse response, can be written as

$$h_p(t) = a_p \frac{\prod_{q=0}^{N-1} \sin(\frac{\pi}{T}(t + t_p - t_q))}{\pi t/T} \qquad \text{(C.4)}$$

and $s_p(t)$ is an impulse train of samples as

$$s_p(t) = \sum_{k=-\infty}^{\infty} x_c(kT + t_p)\delta(t - kT - t_p) \qquad \text{(C.5)}$$

4- Now we can express $x_c(t)$ as the below summation

$$x_c(t) = \sum_{p=0}^{N-1} s_p(t) * h_p(t) \qquad \text{(C.6)}$$

As clear the continuous signal is represented as the summation of N, linear time invariant convolutions which can be implemented by N channel filtering operations.

Appendix D

D.1 Modification of equation (4.9)

Equation (4.9) can be stated as

$$\sum_k \sum_i \phi_{ik}\phi_{im}b_{kn} + \sum_k \sum_i \phi_{ik}\phi_{in}b_{km} = \phi_{mn} + \phi_{nm} \tag{D.1}$$

Using the fact that both B and Φ are symmetric, we can manipulate it as follows

$$\sum_k b_{kn}(\sum_i \phi_{ik}\phi_{im}) + \sum_k b_{km}(\sum_i \phi_{ik}\phi_{in}) = \phi_{mn} + \phi_{nm} \tag{D.2}$$

swap the index of coefficients ϕ_{ik} into ϕ_{ki}, without affecting the result

$$\sum_k b_{kn}(\sum_i \phi_{ki}\phi_{im}) + \sum_k b_{km}(\sum_i \phi_{ki}\phi_{in}) = \phi_{mn} + \phi_{nm} \tag{D.3}$$

Now let the summations inside the parentheses be named as c_{km} and c_{kn}, hence we have

$$\sum_k b_{kn}c_{km} + \sum_k b_{km}c_{kn} = \phi_{mn} + \phi_{nm} \tag{D.4}$$

once more swapping the coefficients in the summations to get

$$\sum_k b_{nk}c_{km} + \sum_k b_{mk}c_{kn} = \phi_{mn} + \phi_{nm} \tag{D.5}$$

Now if we define the B matrix as with elements b_{mn} and C matrix with elements c_{mn} and Φ matrix with elements ϕ_{mn} and use the symmetry fact we can see the following, row n of B is multiplied by column m of C, thus it represents the matrix multiplication of C with B. Therefore (D.1) actually represents the equation below

$$2CB = 2\Phi$$

where C can be found to satisfy $C = \Phi^2$, which directly follows from definition in (D.4). Henceforth equation (4.9) can be written as the matrix multiplication stated below

$$CB = \Phi \tag{D.6}$$

Where C_{LxL} the coefficient matrix derived from Φ as $C = \Phi^2$ (D.7)

The trivial solution of (D.1) is obviously

$$B = C^{-1}\Phi = \Phi^{-1}$$

Which corresponds to nothing but the Yen 4 interpolator. This solution is also equivalent to k=L solution of the trade off.

Now what remains is to show how to modify (D.6) according to a given k. By introducing the k parameter into (D.6) what is meant is that a number of diagonals of B is set to zero by default. However when seeking a solution to (D.6), the complete B matrix is an unknown and the effect of zero elements should be incorporated to C matrix as follows.

Modified C matrix:

C_k is the modified C matrix according to k parameter. The modification is shown below:

Let

$$C = \begin{bmatrix} c_{11} & c_{12} & . & . & . & . & c_{1L} \\ c_{21} & c_{22} & c_{23} & & & & . \\ . & c_{32} & c_{33} & & & & . \\ . & & . & & . & & . \\ . & & & . & c_{ii} & . & . \\ . & & & & . & . & c_{(L-1)L} \\ c_{L1} & . & . & . & . & . & c_{LL} \end{bmatrix}$$

With all coefficients defined according to (D.7). For a given k, C should be multiplied term by term with the following mask to get the modified C_k.

Mask is an LxL binary matrix with the elements defined as follows

$$M(i,j) = 0 \quad \text{if} \quad |i-j|+1 > \text{k}$$

$$M(i,j) = 1 \quad \text{if} \quad |i-j|+1 \le k$$

Hence M will take the following form for given k =3 and L=7 values.

$$M_k = \begin{bmatrix} 1 & 1 & 1 & 0 & 0 & 0 & 0 \\ 1 & 1 & 1 & 1 & 0 & 0 & 0 \\ 1 & 1 & 1 & 1 & 1 & 0 & 0 \\ 0 & 1 & 1 & 1 & 1 & 1 & 0 \\ 0 & 0 & 1 & 1 & 1 & 1 & 1 \\ 0 & 0 & 0 & 1 & 1 & 1 & 1 \\ 0 & 0 & 0 & 0 & 1 & 1 & 1 \end{bmatrix}$$

Therefore the modified C matrix is defined as $C_k = C * M$ where subscript k denotes the effect of k on the C and star is used to indicate that the multiplication is term by term. Equation (4.9) should be modified as follows

$$C_k B = \Phi$$

(D.8)

As the final step the corresponding trade off interpolation coefficients b_{mn} are obtained from the solution of (D.8) as follows:

$$B = C_k^{-1}\Phi \qquad \text{(D.9)}$$

However note that since B matrix is constrained by k, not all the elements of the solution matrix are required. To compensate the calculation of interpolation equation (4.6) B matrix can be masked with M_k. And then the final interpolation coefficients can be written as follows

$$B_k = B * M_k \qquad \text{(D.10)}$$

D.2 Finding optimal k of equation (4.10)

The k value that optimizes the performance of trade-off interpolator was as the value that minimizes the following equation

$$\varepsilon(k) = \sqrt{1 - \lambda_{\min}(k) + tr(k)10^{-\frac{SNR}{10}}}$$

Where $\lambda_{\min}(k)$ is the minimum egienvalue of matrix $2\Phi B_k - (\Phi B_k)^2$ and tr(k) is defined as $tr(\Phi B_k \Phi)$. As obvious all these use matrix B_k to be computed and are lengthy calculations and, are not fitting into a reason of practice. However, even a little bit improvement can occur if for the search of the optimal k, if the masking method is used with a fast mask generator. Only one mask should be generated by a loop and, the remaining operations are carried out with much faster matrix operations. Considering the generation of a mask the pure algorithm uses as much as N^2 times more operations for each masking, if a mask is not employed.